THERMO-CHEMICAL ANALYSES OF THE DRIFT SCALE HEATER TEST: MINERALOGICAL AND GEOCHEMICAL CHARACTERICS

William Glassley
Lawrence Livermore National Laboratory

Level 4 Milestone SP9320M4
WBS 1.2.3.14.2
Summary Account TR3E2FB23

Executive Summary

Reactive transport simulations were conducted of the heating phase of the drift scale heater test. The purpose of the simulations was to determine where, and to what extent, mineralogical changes would occur in response to movement of condensate water, and how the chemical composition of the water would evolve through time. The simulations were conducted using the temperature and flow fields generated using the NUFT code simulations of the thermo-hydrological evolution of the rock surrounding the drift and wing heaters.

Initial simulations indicated that no perceptible changes in mineralogy would occur during the first four years, for those regions within which the temperature did not exceed 40°C. In addition, the region where temperatures exceed 100°C will be regions within which mineralogical changes will be dominated by either mineralogical dehydration, or vapor-phase alteration of existing mineral phases. Hence, the simulations conducted here consider those regions within which temperatures remained between 40°C and 100°C. In the simulations it was assumed that the coexisting gas phase was buffered to a CO_2 pressure of 0.01 bars, consistent with results obtained from the Single Heater Test.

The simulations were conducted for two separate domains (designated Zones 1 and 2). Zone 1 is that region above the heated drift region, that encloses the temperatures of interest, and Zone 2 is the corresponding region below the heated drift. The simulations were conducted in 2-dimensions, along a plan that encompasses the geochemical

9809240206 980922
PDR WASTE
WM-11 PDR

boreholes. Thus, the results provide an indication of the chemical changes in condensate water that may be expected during the course of the heating phase of the system, and of the mineralogical evolution that may occur, as well.

The results demonstrate that large variation in water chemistry should be anticipated, with concentrations of individual cations varying by several orders of magnitude within each zone. This strong compositional zoning of the waters reflects the effect that flow path length has on reaction progress; those regions over which flow distances are short generate dilute waters, while solutions in those regions father along the flow path reach saturation in a variety of secondary minerals.

Secondary mineral development is complex, and depends upon spatial location relative to the drift and wing heaters, and upon time. The saturation state of the waters varies, but indicates that precipitation of secondary minerals should be expected above and below the drifts. The extent of precipitation is time-dependent, but will be greatest above the drift.

Counteracting the effects of mineral precipitation is mineral dissolution. This, too, exhibits complex behavior, but is consistently greatest in the immediate vicinity of the boiling front.

During cool down, reversal of the mineralogical sequence development seen during heating, is anticipated. However, nucleation effects and changes in flow pathways and velocities will lead to inhomogeneous development of secondary phases during this period.

DRAFT DISCLAIMER

This contractor document was prepared for the U.S. Department of Energy (DOE), but has not undergone programmatic, policy, or publication review, and is provided for information only. The document provides preliminary information that may change based on new information or analysis, and is not intended for publication or wide distribution; it is a lower level contractor document that may or may not directly contribute to a published DOE report. Although this document has undergone technical reviews at the contractor organization, it has not undergone a DOE policy review. Therefore, the views and opinions of authors expressed do not necessarily state or reflect those of the DOE. However, in the interest of the rapid transfer of information, we are providing this document for your information.

Introduction

As described in the report on thermo-hydrological processes anticipated to develop during the course of the Drift Scale Heater Test, a boiling front and region of condensate formation will migrate outward from the heated region. The condensate will form along fractures and be imbibed into the rock, in regions where full saturation has not been achieved, or will migrate along fracture surfaces. In the latter case, water will dissolve pre-existing mineral phases that line fracture surfaces, potentially reaching saturation in a number of potential secondary mineral phases. If saturation occurs, precipitation of those phases may occur, provided kinetic barriers to nucleation do not inhibit the mineral growth process. This report describes the first suite of simulations conducted to determine the time-dependent chemical and mineralogical changes expected to develop during the course of the heating phase of the heater test. The purpose of these simulations was to provide a first prediction of the chemical and mineralogical changes that may be observed at the locations of the geochemistry boreholes.

Method

The temperature distribution, and vertical and horizontal components of the velocity field were obtained from the NUFT thermo-hydrological simulations, for the plane within which the geochemical boreholes 69, 70, 71, 72 and 73 are located, for times of 1, 2, 3, and 4 years after turn on of the heaters. This approach of taking sequential time slices through the flow field was taken because current reactive transport simulators that account for non-ideal solute and solvent behavior, and realistic dissolution and precipitation kinetics, generally do not update thermal and flow fields automatically; code enhancements to accomplish this are planned.

The data were fit to a regular mesh of 1 meter x 1 meter grid blocks. Vertical boundaries of the mesh were located at the access drift (approximately 28 meters from the drift center), and at the approximate outer edge of the outer wing heaters. This geometry provided coverage of those regions intersected by the geochemistry boreholes.

Initial, scoping simulations demonstrated that those regions where temperatures were below 40°C, were regions within which there would be virtually no detectable changes in the mineralogy. In addition, for conditions above boiling, existing reactive transport codes have limited capabilities to model fluid-rock interaction. Hence, domains were selected above (Zone 1)

and below (Zone 2) the heated region where temperatures were between 40°C and 100°C, and the simulations were conducted for the flux fields within these regions (see Figures 1, 2 and 3).

The volumetric fluxes (Figure 3), in units of meters^3 of /year, were generated by reformulating the thermo-hydrologically computed vertical and horizontal velocity components using the following relationships:

$$V = Q / (\phi_m(1-\phi_f) + \phi_f),$$

where V is the fluid velocity, Q is the volumetric flux and, ϕ_m and ϕ_f are the matrix and fracture porosity, respectively, per unit rock volume. Generally, ϕ_m is much greater than ϕ_f, thus allowing the simplification that

$$V = Q / \phi_m$$

and

$$V_f = Q / \phi_f ,$$

where V_f is the fracture velocity. For the case where the fracture flux is much greater than the matrix flux, this relationship can be recast as

$$Q_f = ((\phi_m/\phi_f)V_z)*(1.48219e10 \text{ secs/year}),$$

where Q_f is the volumetric fracture flux, per unit cross sectional area (meter^2 of cross-sectional area), and V_z is the velocity component in the x or z direction.

The calculations were conducted assuming that the instantaneous flow field and temperature field obtained from the thermo-hydrological modeling, at each selected time, represented a reasonable approximation for the time-averaged flow and temperature fields for the preceding year. This approximation can over-estimate the extent of reaction at each grid block, since it assumes that each grid block experiences the defined temperature and flow field for 12 months. In reality, each location represented by the grid blocks will see a progressive change in conditions for the duration of the DST. To evaluate the extent to which this approach would provide misleading results, simulations for each year were conducted assuming that the conditions persisted for 0.1 years, 1, 2, 3, and 4 years, and the results compared. The results of these comparisons are described below.

For each year for which simulations were conducted, the initial mineralogy was the same. This approach allows the specific effects due to the evolution of the physical parameters (temperature and flow fields) to be determined. Future simulations will consider the effects of mineralogical changes that occur due to heat and fluid transfer during preceding years.

The initial mineralogy was assumed to be that which appears to be responsible for development of the compositional characteristics of water collected from Hole 16 of the Single Heater Test (Glassley and DeLoach, 1997). The mineralogy was that typical of fractures (calcite, cristobalite, kaolinite [a proxy for complex smectite/illite clays]), but also allowing for minor interaction with the Tsw2 matrix (albite and K-feldspar [proxies for alkali feldspar], quartz and cristobalite).

Particular attention was focused on the concentrations of those solutes that usually account for ca 90% of the total dissolved solids normally encountered in waters in fractures and in the saturated zone at Yucca Mountain (i.e., Ca^{++}, Na^{+}, K^{+}, SiO_2, Al^{+++}, and HCO_3^{-}), and on those mineral phases that either compose the rock (i.e., cristobalite, quartz, K-feldspar, albite, calcite) or which may reasonably be expected to occur as secondary minerals during reaction progress for the period of time the test is ongoing (i.e., chalcedony, kaolinite, diaspore, stilbite). Porosity changes, pH, and the concentrations of other solute species were also considered in the calculations.

The code used in the simulations was GIMRT (Steefel and Yabusaki, 1995), which allows direct monitoring of changes in porosity, solution composition, and dissolution or precipitation of mineral phases, as a function of temperature, pressure, fluid flux, input solution chemistry, reaction kinetics, and system geometry.

Initial water chemistry was assumed to be that of condensate in equilibrium with 0.01 bars of CO_2. Condensate was modeled as containing 1.0e-10 moles of each basis species, at a pH of 6.85 and HCO_3^{-} molality of 7.11e-6.

Mineralogical development during cool down was initially simulated in thermal fields in which temperatures decreased along the flow pathway. However, it was quickly evident that such simulations will not represent the effects of cool down, since experience has shown that nucleation effects dominate mineral development during rapid temperatrure drops, as expected in the DST. As a result, we anticipate that the mineralogical sequence developed during progressive heating will be reversed, but the extent of mineralogical development will be small, and supersaturated fluids will develop.

Results

Comparison of pH distribution (Figure 4) at 0.1 and 1.0 years in Zone 1 shows that there is very little difference in the absolute values of pH over this time period. Since dissolution and precipitation of the solid minerals is modeled as a series of simultaneous hydrolysis reactions, the similarities between the pH distributions in these two time periods is mimicked by the cation and ion distribution of other species. Hence, it was decided to conduct simulations for 1 year duration, at the time periods considered. These results will then provide a conservative indication of the solution chemistries that may be encountered in the geochemistry holes. Conservative is used in this context as being a result that overestimates the extent of mineral dissolution and/or precipitation.

Simulations conducted for all time periods showed that the chemical and mineralogical changes were smoothly continuous for the duration of the heating period. Hence, only the results for the first and fourth years are presented, as they provide a thorough description of the effects to

be expected in the evolution of the geochemical and mineralogical system. As the evolution is different between Zones 1 and 2, the characteristics of these zones will be discussed separately.

Zone 1

In general, the changes in solution chemistry and mineral distributions directly reflect the flux vectors. The greatest vertical fluxes of heated water occur immediately above the central drift, and to a lesser extent immediately over the wing heaters. Within these areas dissolution of primary minerals is the greatest. Since this is an area within which the path length is relatively short, it is also the region in which the concentrations of dissolved species are consistently the lowest (see Figures 5, a-d, and 6, a-d).

During the first year of heating, all dissolved basis species exhibit a ridge of maximum concentration within the upper half of Zone 1. This phenomenon reflects the fact that the solution achieves saturation in calcite, kaolinite and stilbite by this point along the flow path. For all of the species, solution composition varies by several orders of magnitude along the flow path, which is a sufficiently large contrast to allow detection by the analytical methods expected to be used in analysis of collected fluids.

During the fourth year, the solute distribution patterns are more complex, although the general tendency toward more dilute concentrations nearest the heaters persists. Ca^{++} maintains a broad compositional ridge in the middle portion of Zone 1, while K^+ and SiO_2 (aqueous) develop smoothly increasing concentration profiles away from the heaters. Na^+ develops regions of very low concentration over the wing heaters in the middle distance within the zone, which punctuate the otherwise regular increase in Na^+ away from the heaters.

The saturation state of the mineral phases is indicated by the saturation index, which is defined as the log of the ratio of the ion activity product (Q) of the respective hydrolysis reaction to the equilibrium constant (K) of the hydrolysis reaction (i.e., log[Q/K]). Values of the saturation index that are greater than zero indicate that the solution is supersaturated in the mineral phase, while values less than zero are undersaturated. Because of uncertainty associated with thermodynamic parameters used in the calculations, it is generally considered that saturation indices within 0.1 log units of zero indicate an equilibrium or saturated conditioned.

Consideration of the saturation indices for the first year of heating (Figure 7, a-f) indicate that the solution becomes saturated to supersaturated in calcite, kaolinite and stilbite in some regions within zone 1, and is consistently undersaturated in quartz, potassium feldspar and albite throughout zone 1. By the fourth year (Figure 8, a-f), most of the area within zone 1 is saturated or supersaturated with respect calcite, K-feldspar, quartz and stilbite, but remains undersaturated in albite. Kaolinite is generally undersaturated throughout the zone, with the exception of a central ridge running through the zone where the water is nearly saturated in kaolinite.

For all time periods considered, there is a net porosity increase at the base of the boiling zone, changing from an initial 2.75% to approximately 3.2-3.4%. From this maximum porosity, there is a steady and smooth decrease in absolute porosity, moving outward toward cooler regions. Nevertheless, during the first year, the porosity remains above that of the initial state for the entire area of Zone 1. However, by the fourth year, there is sufficient development of secondary mineral phases in the coolest regions of the zone, to result in a net decrease in porosity below that of the initial state, down to approximately 2.6%.

Zone 2

As in Zone 1, the changes in solution chemistry and mineral distributions correspond to the flux vectors. Immediately below the central drift, and to an even greater extent immediately below the wing heaters, large downward fluxes develop . As observed in Zone 1, these are areas where dissolution of primary minerals is the greatest because the condensate flow path lengths are relatively short and the concentrations of dissolved species are consistently the lowest (see Figures 9, a-d, and 10, a-d).

As a result, all dissolved basis species exhibit an increase in concentration with distance away from the heated region. By the fourth year, this pattern is strongly influenced by the high fluxes immediately below the wing heaters, which results in an apparent bulge in the concentration contours in the lower middle portion of the zone. For all of the species, solution composition varies by several orders of magnitude along the flow path, which is a sufficiently large contrast to allow detection by the analytical methods expected to be used in analysis of collected fluids.

Consideration of the saturation indices for the first year of heating (Figure 11, a-f) indicate that the solution becomes saturated to supersaturated only in kaolinite and stilbite in lower and central regions, respectively, within zone 2, and is consistently undersaturated in quartz, potassium feldspar and albite throughout zone 2. By the fourth year (Figure 12, a-f), calcite saturation is achieved within the central region of Zone 2, directly below the central drift, as with kaolinite and stilbite. The zone remains undersaturated in albite and K-feldspar.

As in Zone 1, there is a net porosity increase at the edge of the boiling zone, changing from an initial 2.75% to approximately 3.4%. From this maximum porosity, there is a steady and smooth decrease in absolute porosity, moving outward toward cooler regions. However, unlike Zone 1, there is no region within the zone area where the porosity decreases below initial values.

Discussion and Conclusion

These results indicate that significant changes in solution composition can be expected and detected during the course of the heating period of the Drift Scale Heater Test. These changes are expected to evolve as a function of time and location with respect to the wing heaters and central

drift. It is clear by comparing the results from the different time intervals, that the duration of the experiment must be a minimum of 4 years, in order for the changes to occur along fracture surfaces in a manner that will allow thorough characterization of dissolution and precipitation effects.

These preliminary results suggest that mineralogical changes may be of such magnitude as to result in detectable modification of fracture apertures. Both above and below the drift, a complex history of mineral dissolution and precipitation can be expected. Above the heated region, calcite can be expected to precipitate, along with clay and zeolite. However, the progressive changes in the thermal and flow regimes will cause early precipitated phases to experience later dissolution in some areas, and reprecipitation at later times in other areas. Below the heated region, similar effects are expected, but the geometry is not a mirror image of that above the heaters. Instead, because of the thermal load placed on the system by the wing heaters, mineral precipitation may be concentrated immediately below the central drift. Under most conditions within the studied zones, the primary alkali feldspar components are undersaturated, and are expected to exhibit dissolution effects. Calcite, however, which is the dominant fracture lining mineral, will record a complex history of dissolution and precipitation.

During cool down, collapse of the rehydration front is slow, relative to the thermal field evolution. As a result mineralogical changes will be concentrated in an environment within which temperatures are falling, and fluid velocities are dropping. Consequently, it is theoretically possible that changes in mineralogy during the cool down phase will represent reversal of the reactions that progressed during the heat-up phase. However, experience has shown that nucleation of secondary phases during cool down of experimental systems does not usually follow an equilibrium pathway. This primarily reflects the difficulty of overcoming nucleation energy barriers. As a result, as a first approximation, it is expected that the mineralogical sequence that developed during heat up will be reversed during cool down, but the extent of recrystallization will be insufficient to eliminate the secondary phases formed during heating. In addition, because the flow fields will evolve differently during cool down, it is anticipated that nucleation effects will cause "spotty" distribution of the secondary phase development during cool down.

If these results are supported by later simulations that address the limitations described in the section on "Methods", it may be anticipated that regions above and below the drift will experience significant changes in porosity. These changes may be detectable using a variety of remote sensing techniques, and should be considered in future discussions concerning *in situ* measurements.

References

Glassley, W.E., and Laura DeLoach, 1997, Second Quarter Results of Chemical Measurements in the Single Heater Test. Milestone SP9240M4, Yucca Mountain Project, Lawrence Livermore National Laboratory, Livermore, CA.

Steefel, C.I. and Yabusaki, S.B., 1995. OS3D/GIMRT: Software for modeling multicomponent-multidimensional reactive transport. Pacific Northwest Laboratory, Richland, Washington.

Figure Captions

Figure 1: Respective locations of the geochemistry holes and the modeled regions (Zones 1 and 2). Zone 1 of the 1st and 4th year of heating are shown in blue and red, respectively, above the region of the heaters (located at approximately -250 meters). Zone 2 of the 1st and 4th years of heating are shown in blue and red, respectively, below the region of heating. The origin for the horizontal and distance scales are the same as used inteh thermo-hydrological modeling of the DST.

Figure 2, a, b : The temperature fields for years 1 and 4. The color scales are the same for both years. The horizontal and vertical distances are based on the same zero coordinates as those used in the thermo-hydrological models.

Figure 3, a, b : Flux vectors, at 1 and 4 years. Fluxes are in units of m^3 of fluid/m^2 of cross sectional area/year. The coordinate system is the same as that used in Fig. 2.

Figure 4, a,b : pH in Zone 1 at 0.1 and 1.0 years. See Fig. 1 for the location of the figure origin.

Figure 5, a-d: Distribution of Ca^{++}, K^+, Na^+, and SiO_2(aqueous) aqueous species in Zone 1 during the first year of heating.

Figure 6, a-d: Distribution of Ca^{++}, K^+, Na^+, and SiO_2(aqueous) aqueous species in Zone 1 during the fourth year of heating.

Figure 7, a-f : Saturation index (log Q/K) for the minerals albite, calcite, kaolinite, K-feldspar, quartz, and stilbite, in Zone 1, during the first year of heating.

Figure 8, a-f: Saturation index (log Q/K) for the minerals albite, calcite, kaolinite, K-feldspar, quartz, and stilbite, in Zone 1, during the fourth year of heating.

Figure 9, a-d: Distribution of Ca^{++}, K^+, Na^+, and SiO_2(aqueous) aqueous species in Zone 2 during the first year of heating.

Figure 10, a-d: Distribution of Ca^{++}, K^{+}, Na^{+}, and SiO_2(aqueous) aqueous species in Zone 2 during the fourth year of heating.

Figure 11, a-f : Saturation index (log Q/K) for the minerals albite, calcite, kaolinite, K-feldspar, quartz, and stilbite, in Zone 2, during the first year of heating.

Figure 12, a-f: Saturation index (log Q/K) for the minerals albite, calcite, kaolinite, K-feldspar, quartz, and stilbite, in Zone 2, during the fourth year of heating.

LOCATIONS OF BOREHOLES AND STUDIED ZONES

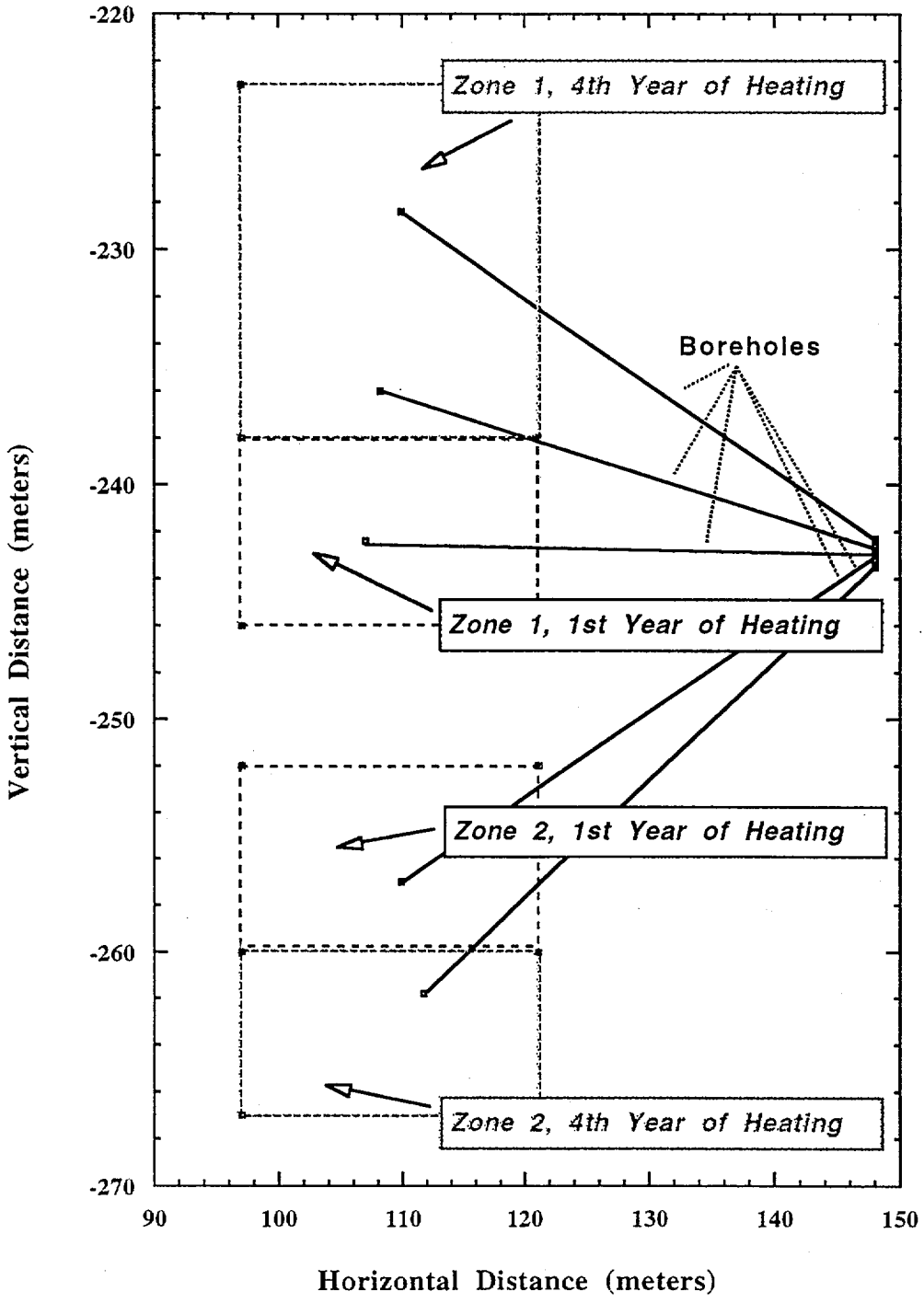

Figure 1

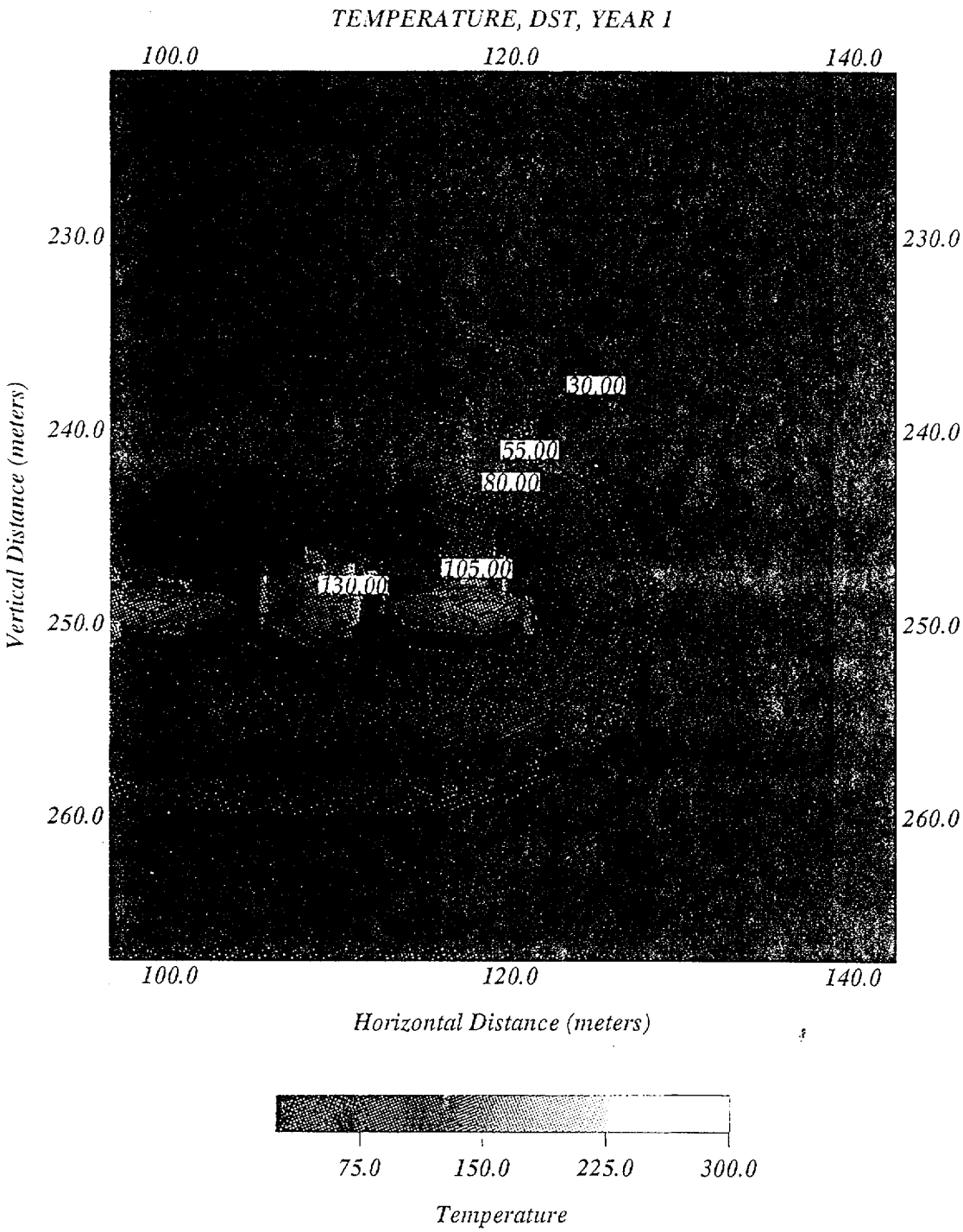
TEMPERATURE, DST, YEAR 1
100.0
120.0
140.0
230.0
240.0
250.0
260.0
Vertical Distance (meters)
30.00
55.00
80.00
105.00
130.00
Horizontal Distance (meters)
75.0
150.0
225.0
300.0
Temperature

Figure 2a

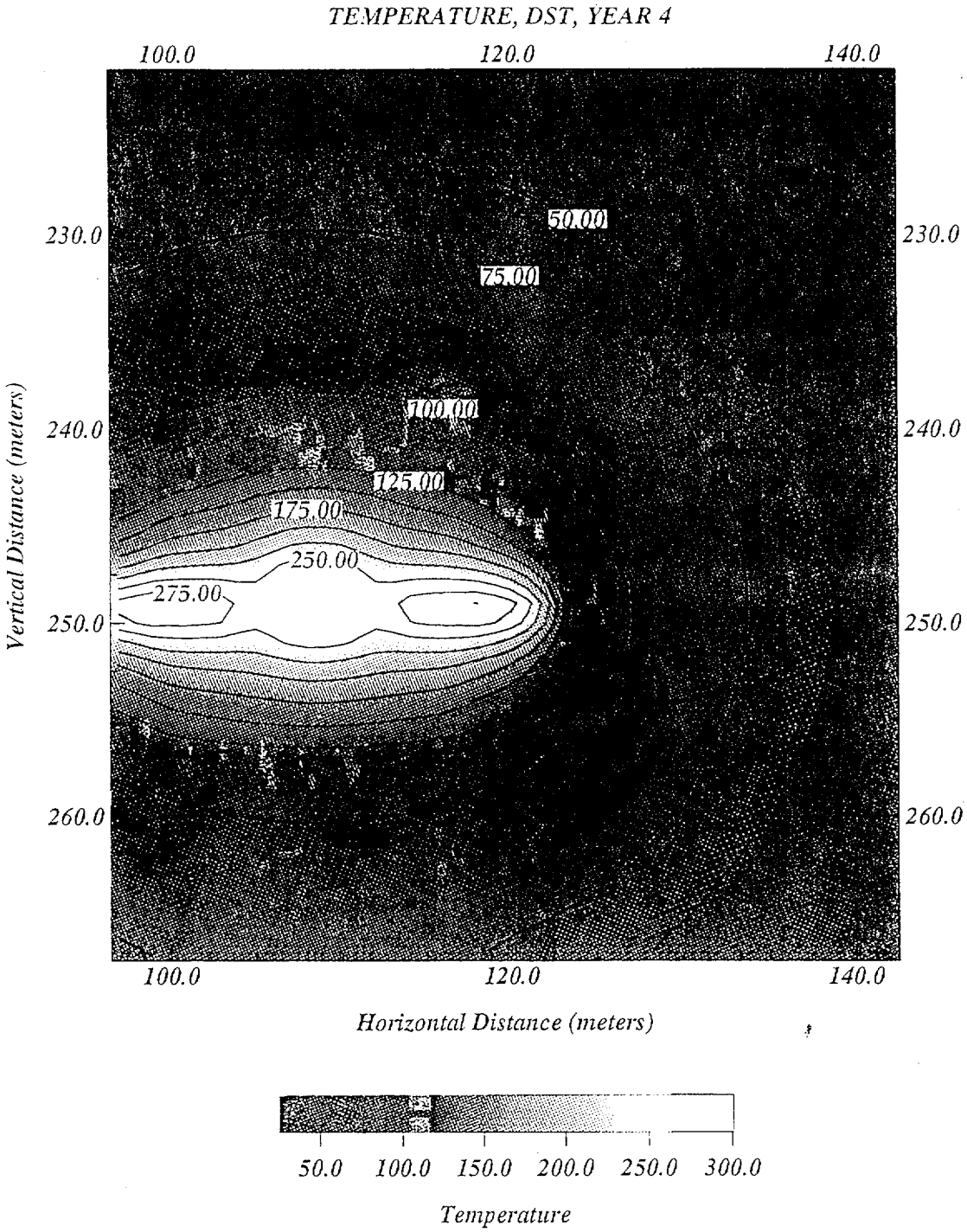
TEMPERATURE, DST, YEAR 4
100.0
120.0
140.0
230.0
240.0
250.0
260.0
Vertical Distance (meters)
50.00
75.00
100.00
125.00
175.00
250.00
275.00
Horizontal Distance (meters)
50.0
100.0
150.0
200.0
250.0
300.0
Temperature

Figure 2b

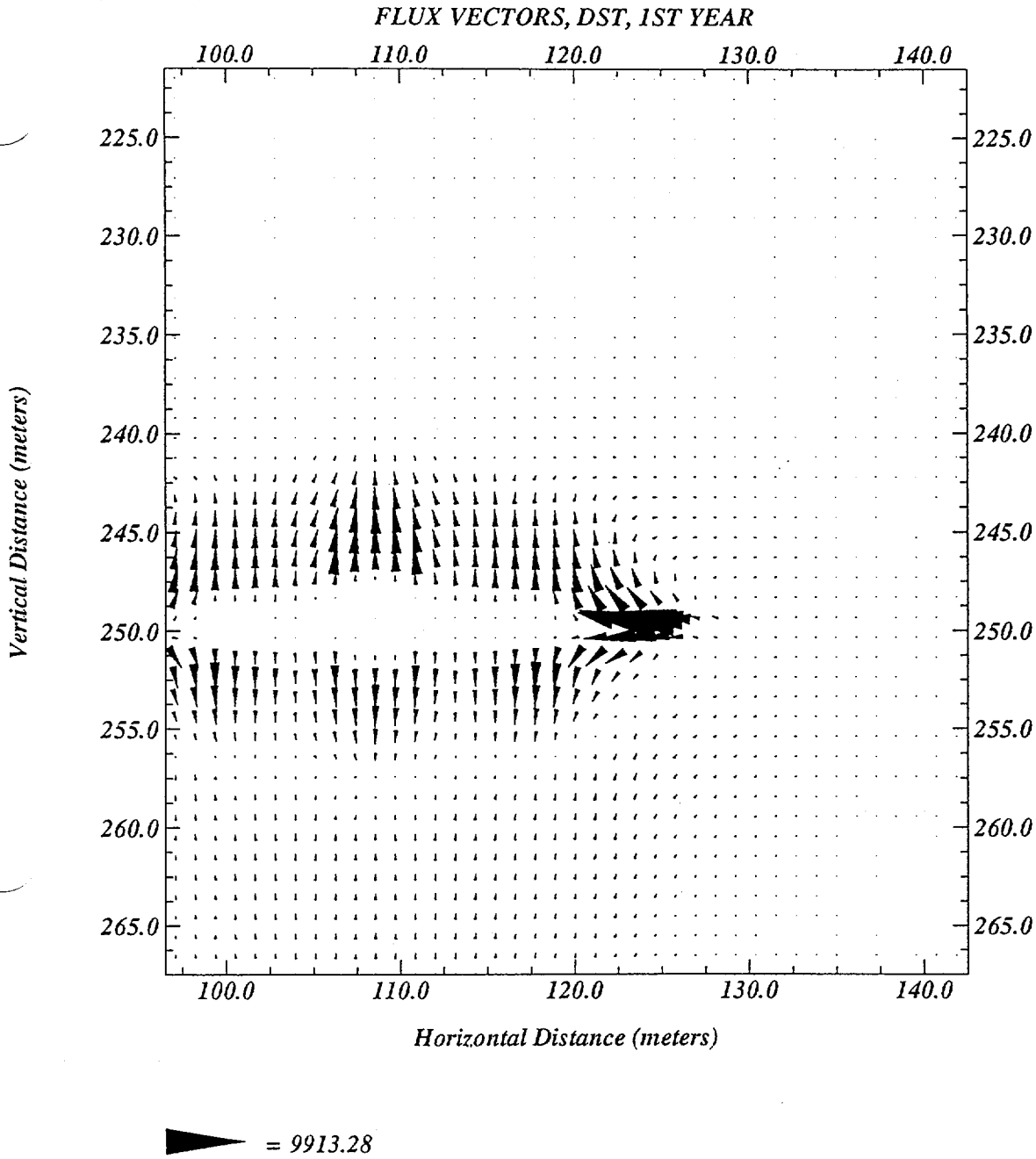
FLUX VECTORS, DST, 1ST YEAR
100.0
110.0
120.0
130.0
140.0
225.0
230.0
235.0
240.0
245.0
250.0
255.0
260.0
265.0
Vertical Distance (meters)
Horizontal Distance (meters)
= 9913.28

Figure 3a

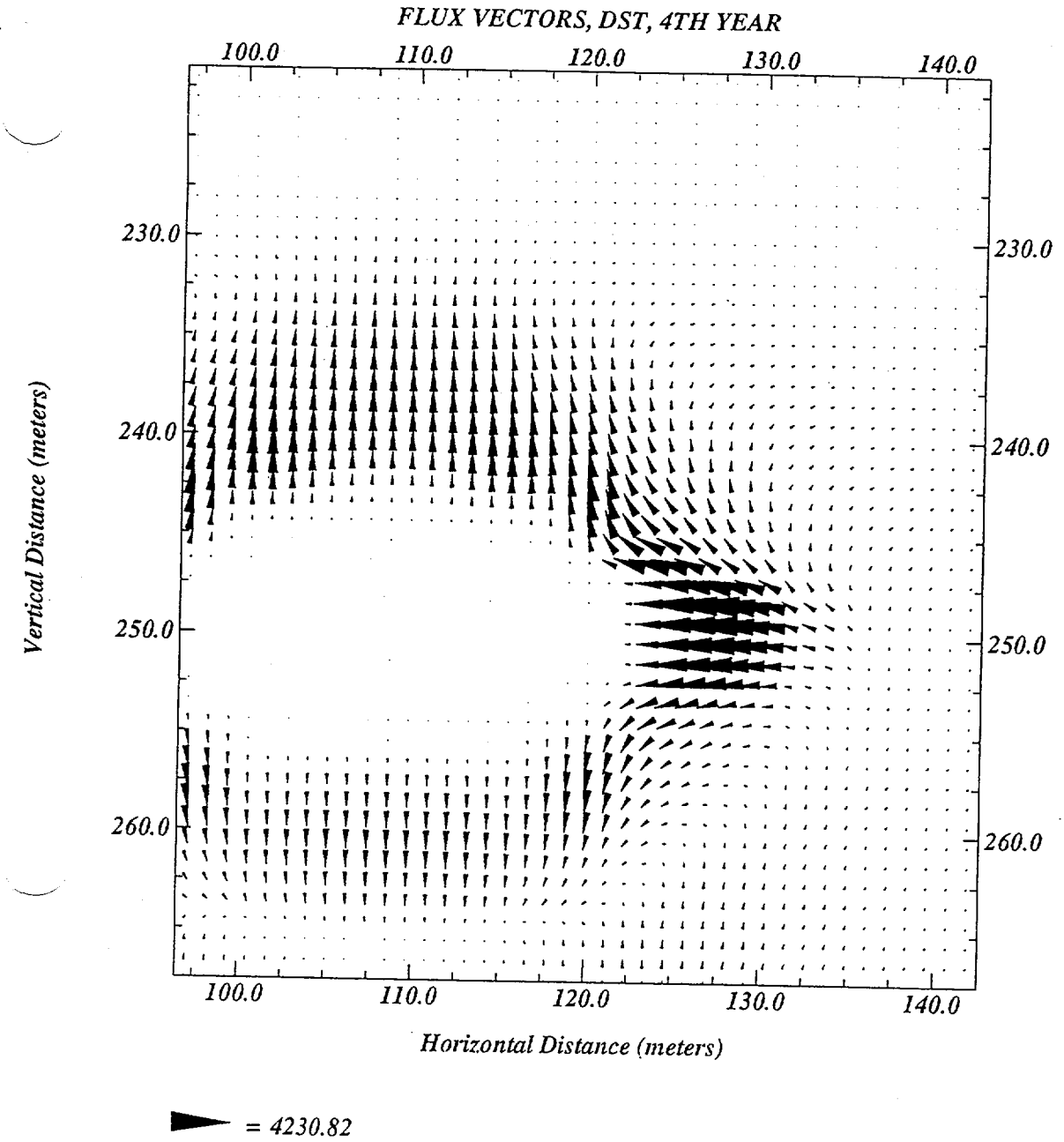
FLUX VECTORS, DST, 4TH YEAR
100.0
110.0
120.0
130.0
140.0
230.0
240.0
250.0
260.0
Vertical Distance (meters)
Horizontal Distance (meters)
= 4230.82

Figure 3b

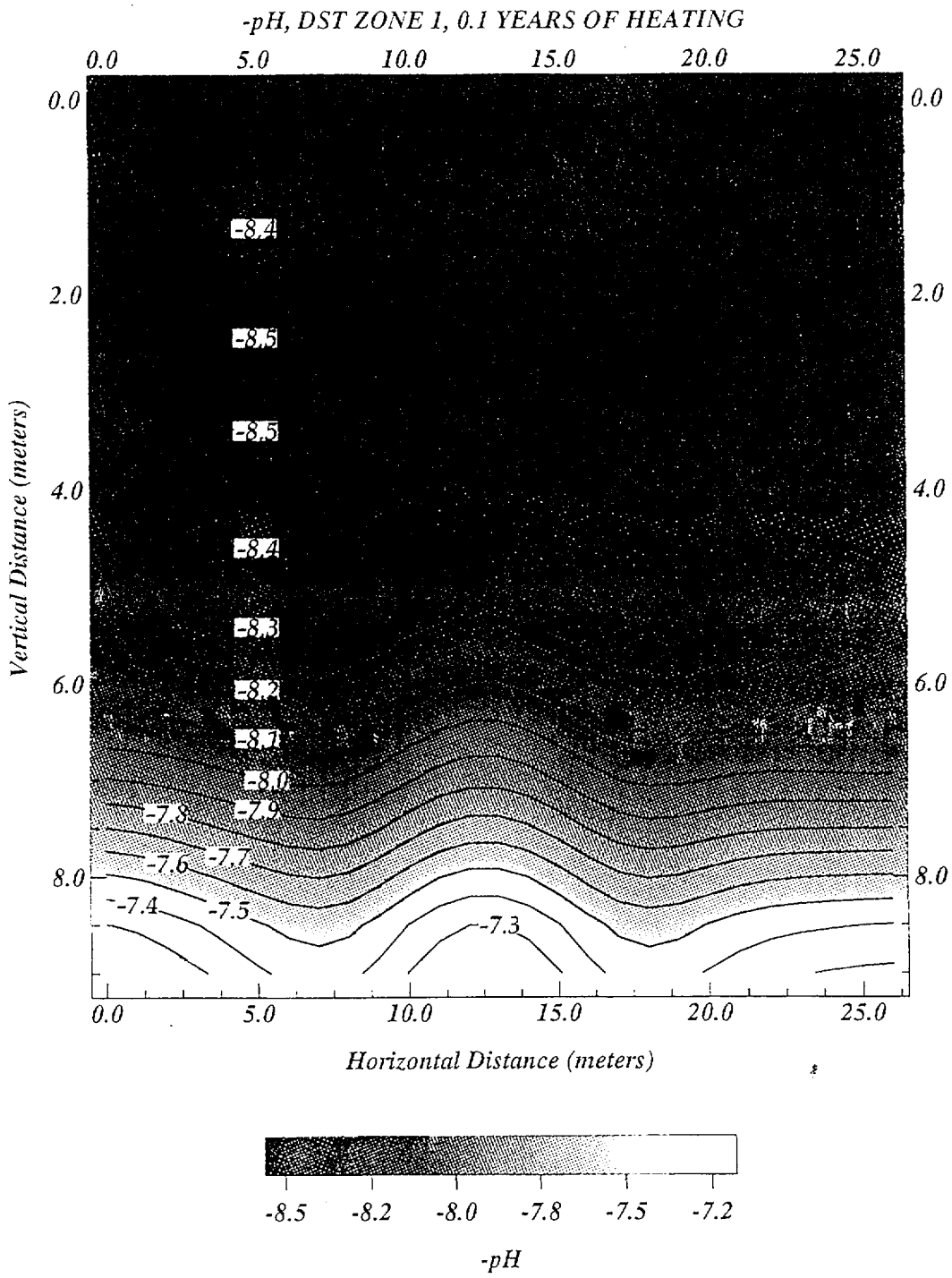
-pH, DST ZONE 1, 0.1 YEARS OF HEATING
0.0
5.0
10.0
15.0
20.0
25.0
0.0
2.0
4.0
6.0
8.0
Vertical Distance (meters)
-8.4
-8.5
-8.5
-8.4
-8.3
-8.2
-8.1
-8.0
-7.9
-7.8
-7.7
-7.6
-7.5
-7.4
-7.3
Horizontal Distance (meters)
-8.5
-8.2
-8.0
-7.8
-7.5
-7.2
-pH

Figure 4a

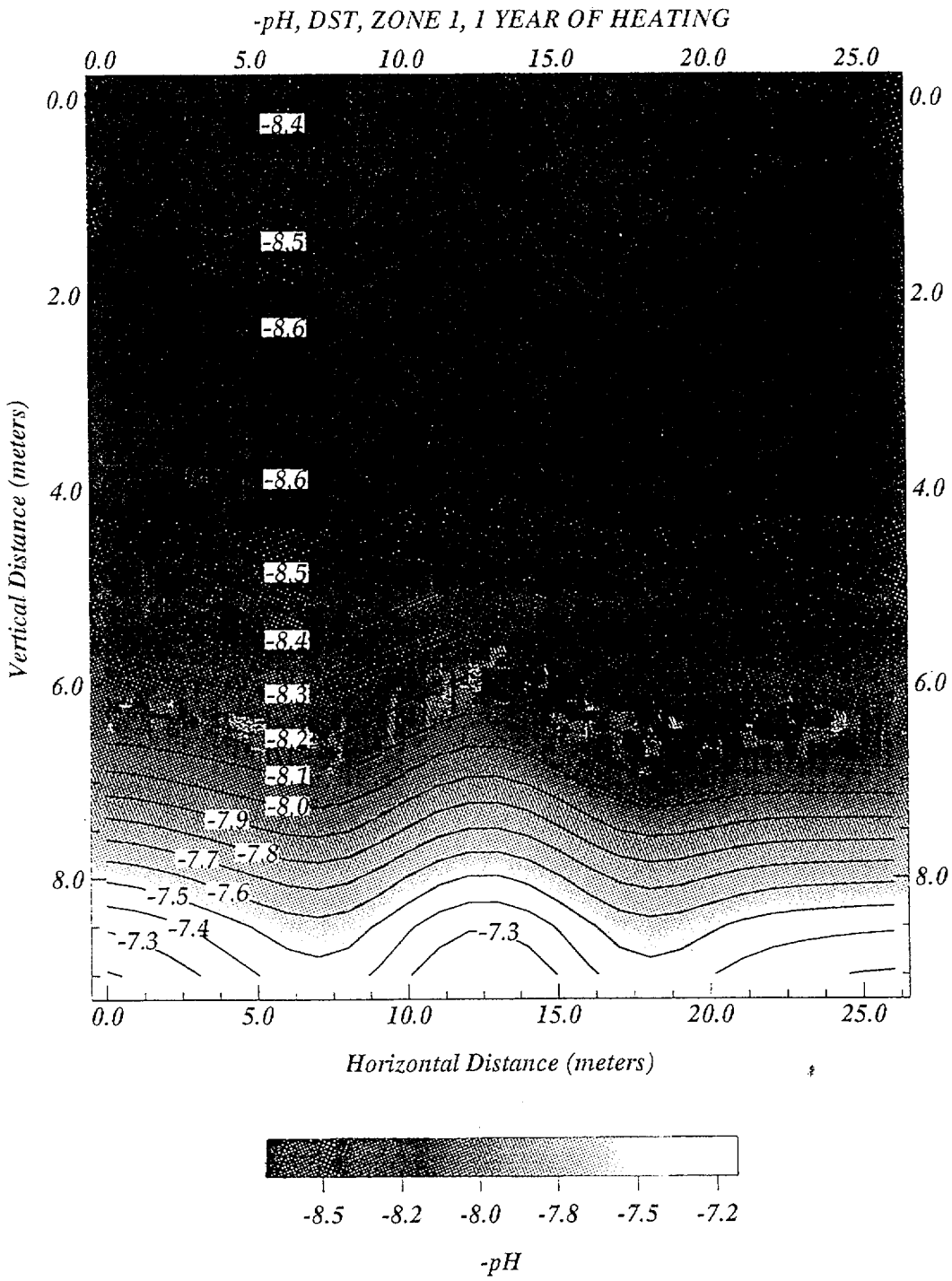
-pH, DST, ZONE 1, 1 YEAR OF HEATING
0.0
5.0
10.0
15.0
20.0
25.0
2.0
4.0
6.0
8.0
Vertical Distance (meters)
-8.4
-8.5
-8.6
-8.6
-8.5
-8.4
-8.3
-8.2
-8.1
-8.0
-7.9
-7.8
-7.7
-7.6
-7.5
-7.4
-7.3
-7.3
Horizontal Distance (meters)
-8.5
-8.2
-8.0
-7.8
-7.5
-7.2
-pH

Figure 4b

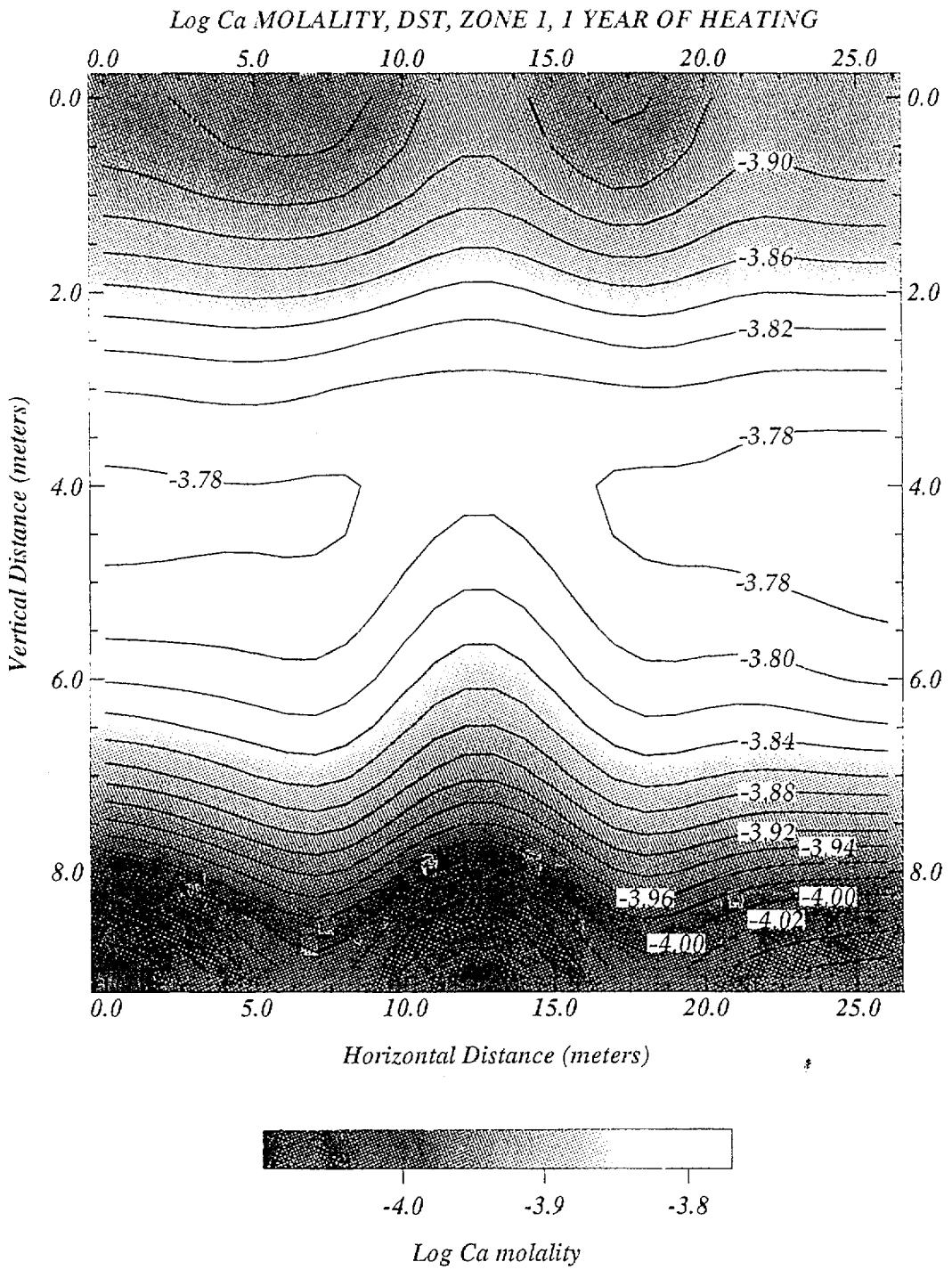
Log Ca MOLALITY, DST, ZONE 1, 1 YEAR OF HEATING
0.0
5.0
10.0
15.0
20.0
25.0
0.0
2.0
4.0
6.0
8.0
Vertical Distance (meters)
-3.90
-3.86
-3.82
-3.78
-3.78
-3.78
-3.78
-3.80
-3.84
-3.88
-3.92
-3.94
-3.96
-4.00
-4.02
-4.00
Horizontal Distance (meters)
-4.0
-3.9
-3.8
Log Ca molality

Figure 5a

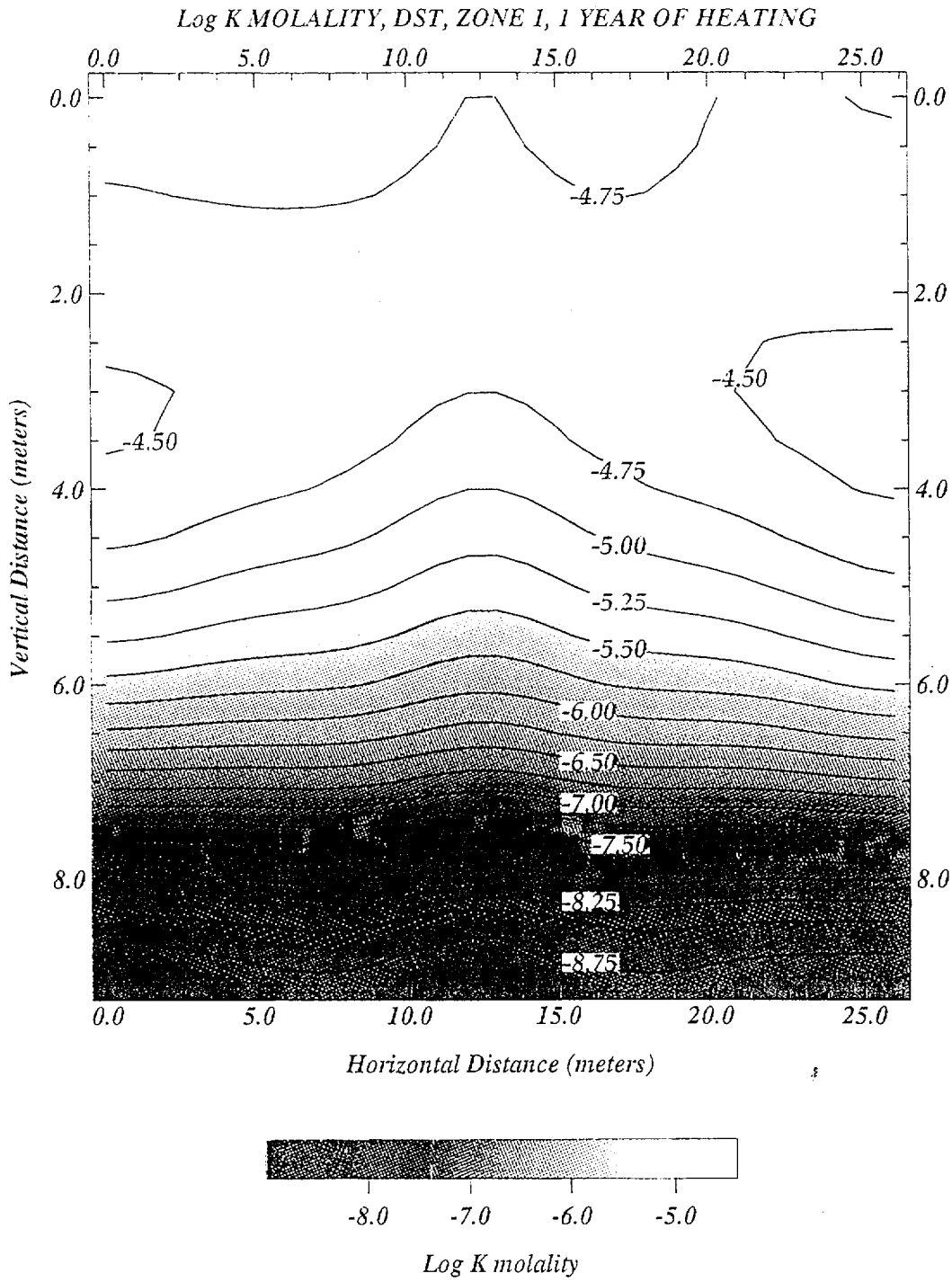
Log K MOLALITY, DST, ZONE 1, 1 YEAR OF HEATING
0.0
5.0
10.0
15.0
20.0
25.0
0.0
2.0
4.0
6.0
8.0
Vertical Distance (meters)
-4.75
-4.50
-4.50
-4.75
-5.00
-5.25
-5.50
-6.00
-6.50
-7.00
-7.50
-8.25
-8.75
Horizontal Distance (meters)
-8.0
-7.0
-6.0
-5.0
Log K molality

Figure 5b

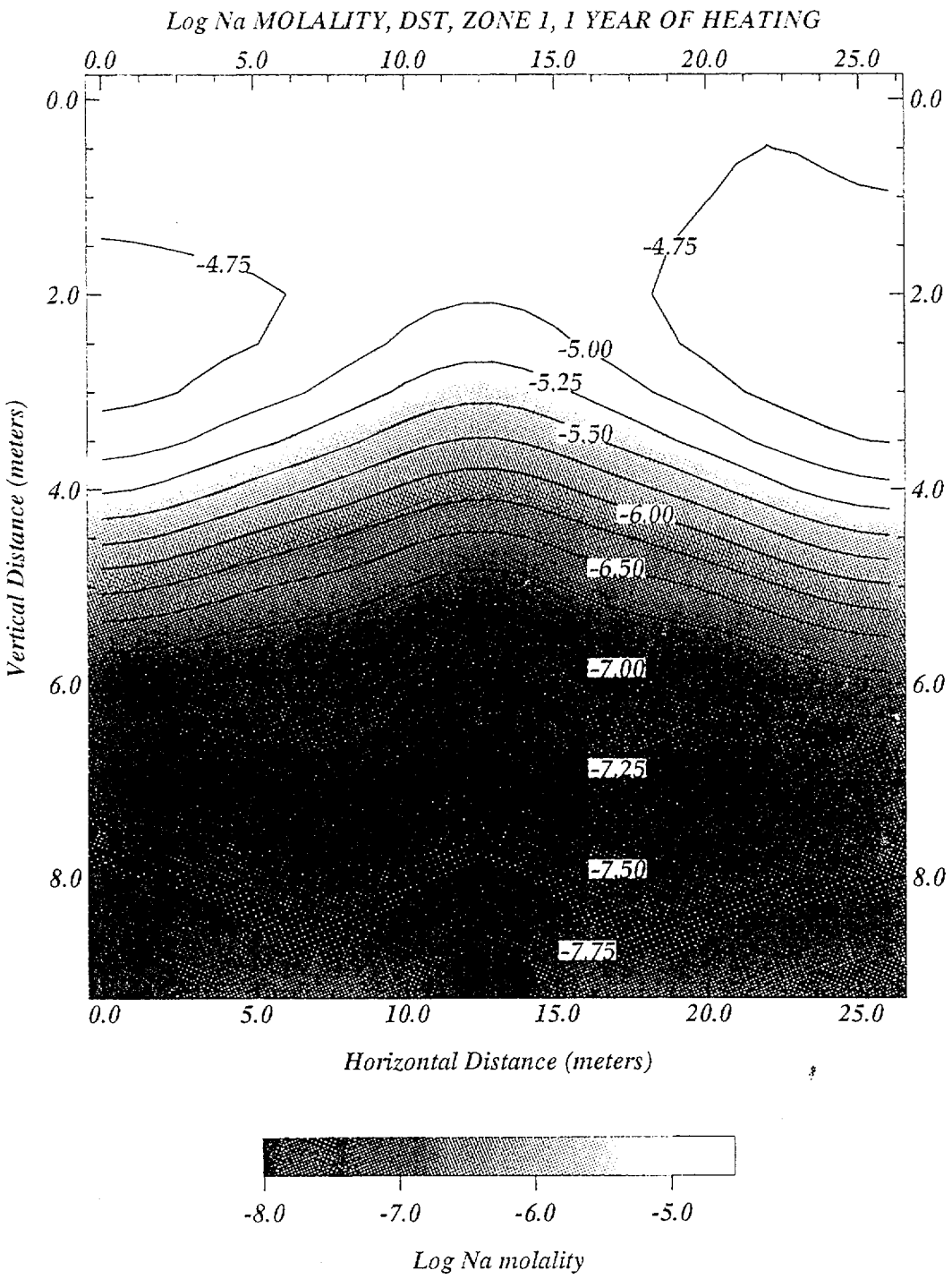
Log Na MOLALITY, DST, ZONE 1, 1 YEAR OF HEATING
0.0
5.0
10.0
15.0
20.0
25.0
0.0
2.0
4.0
6.0
8.0
Vertical Distance (meters)
-4.75
-4.75
-5.00
-5.25
-5.50
-6.00
-6.50
-7.00
-7.25
-7.50
-7.75
Horizontal Distance (meters)
-8.0
-7.0
-6.0
-5.0
Log Na molality

Figure 5c

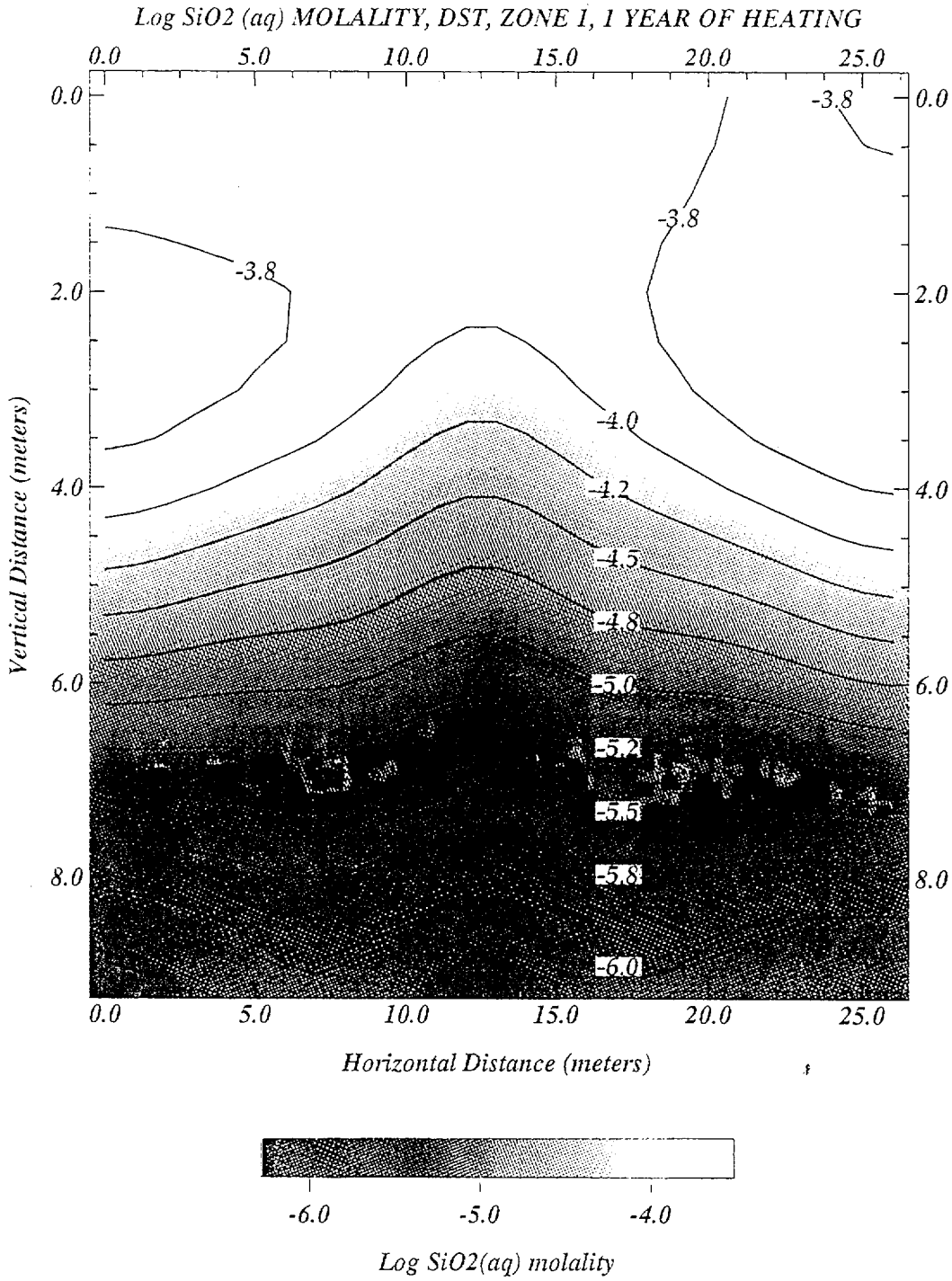
Log SiO2 (aq) MOLALITY, DST, ZONE 1, 1 YEAR OF HEATING
0.0
5.0
10.0
15.0
20.0
25.0
2.0
4.0
6.0
8.0
Vertical Distance (meters)
Horizontal Distance (meters)
-3.8
-4.0
-4.2
-4.5
-4.8
-5.0
-5.2
-5.5
-5.8
-6.0
-6.0
-5.0
-4.0
Log SiO2(aq) molality

Figure 5d

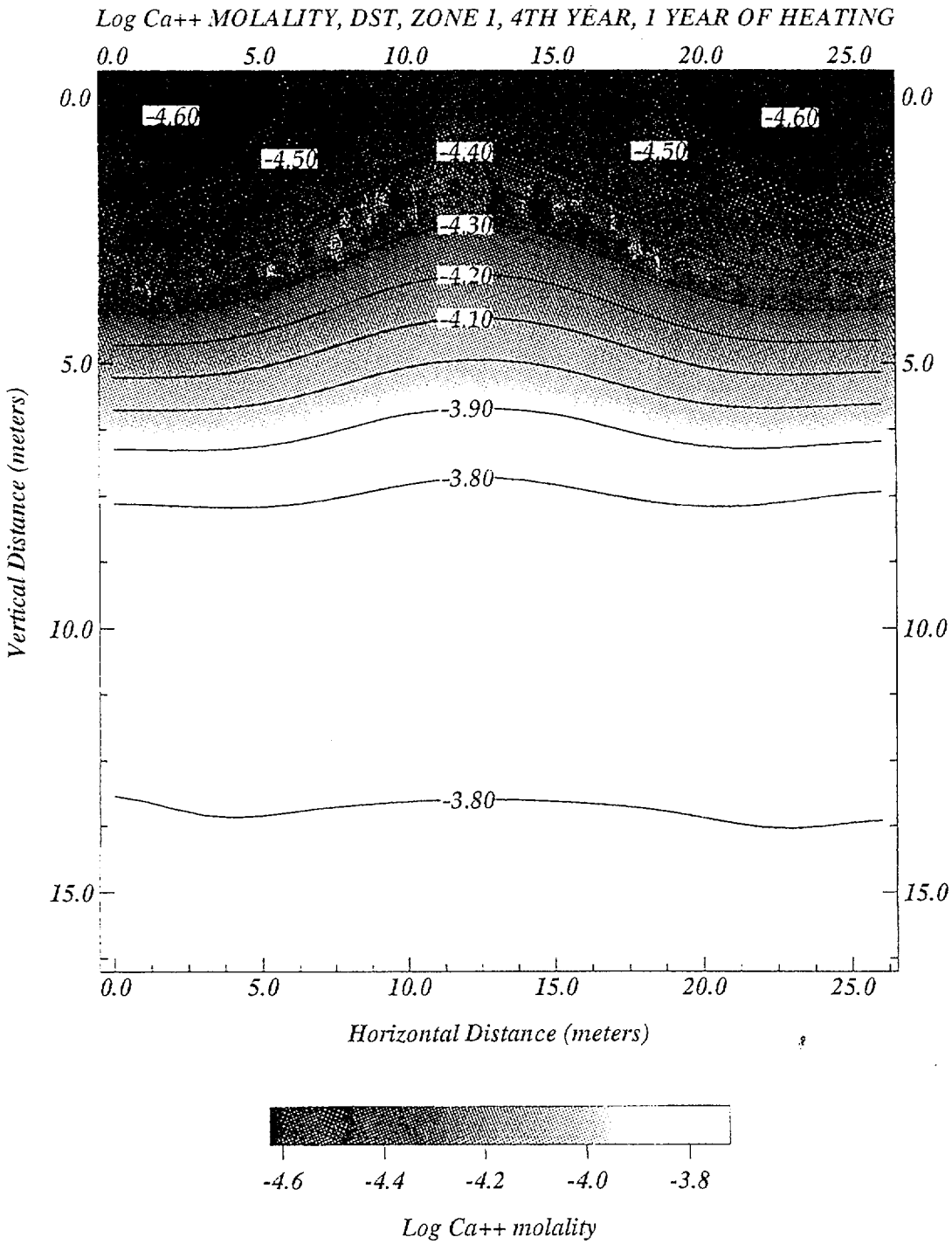
Log Ca++ MOLALITY, DST, ZONE 1, 4TH YEAR, 1 YEAR OF HEATING
0.0
5.0
10.0
15.0
20.0
25.0
-4.60
-4.50
-4.40
-4.30
-4.20
-4.10
-3.90
-3.80
-3.80
Vertical Distance (meters)
Horizontal Distance (meters)
-4.6
-4.4
-4.2
-4.0
-3.8
Log Ca++ molality

Figure 6a

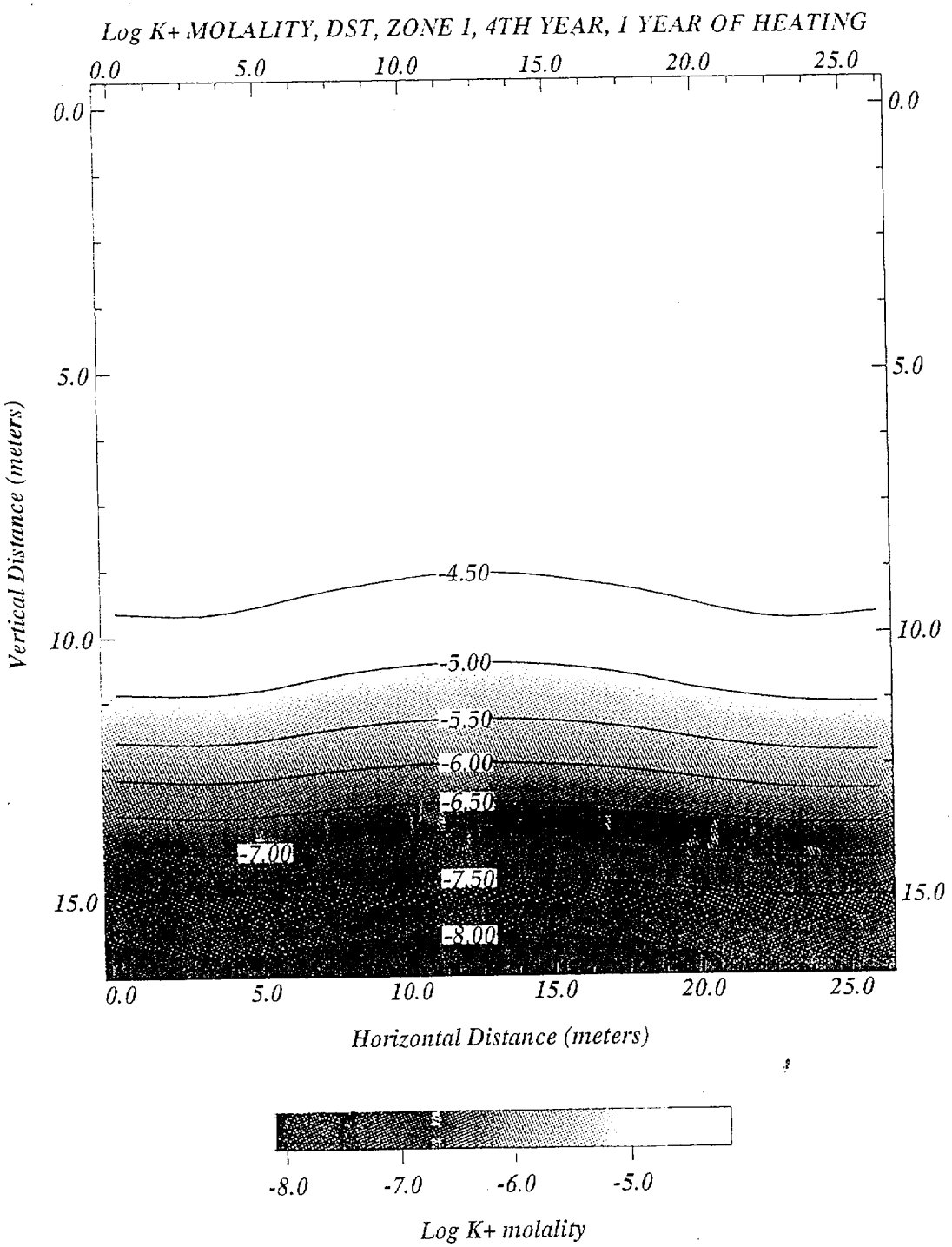
Log K+ MOLALITY, DST, ZONE 1, 4TH YEAR, 1 YEAR OF HEATING
0.0
5.0
10.0
15.0
20.0
25.0
Vertical Distance (meters)
-4.50
-5.00
-5.50
-6.00
-6.50
-7.00
-7.50
-8.00
Horizontal Distance (meters)
-8.0
-7.0
-6.0
-5.0
Log K+ molality

Figure 6b

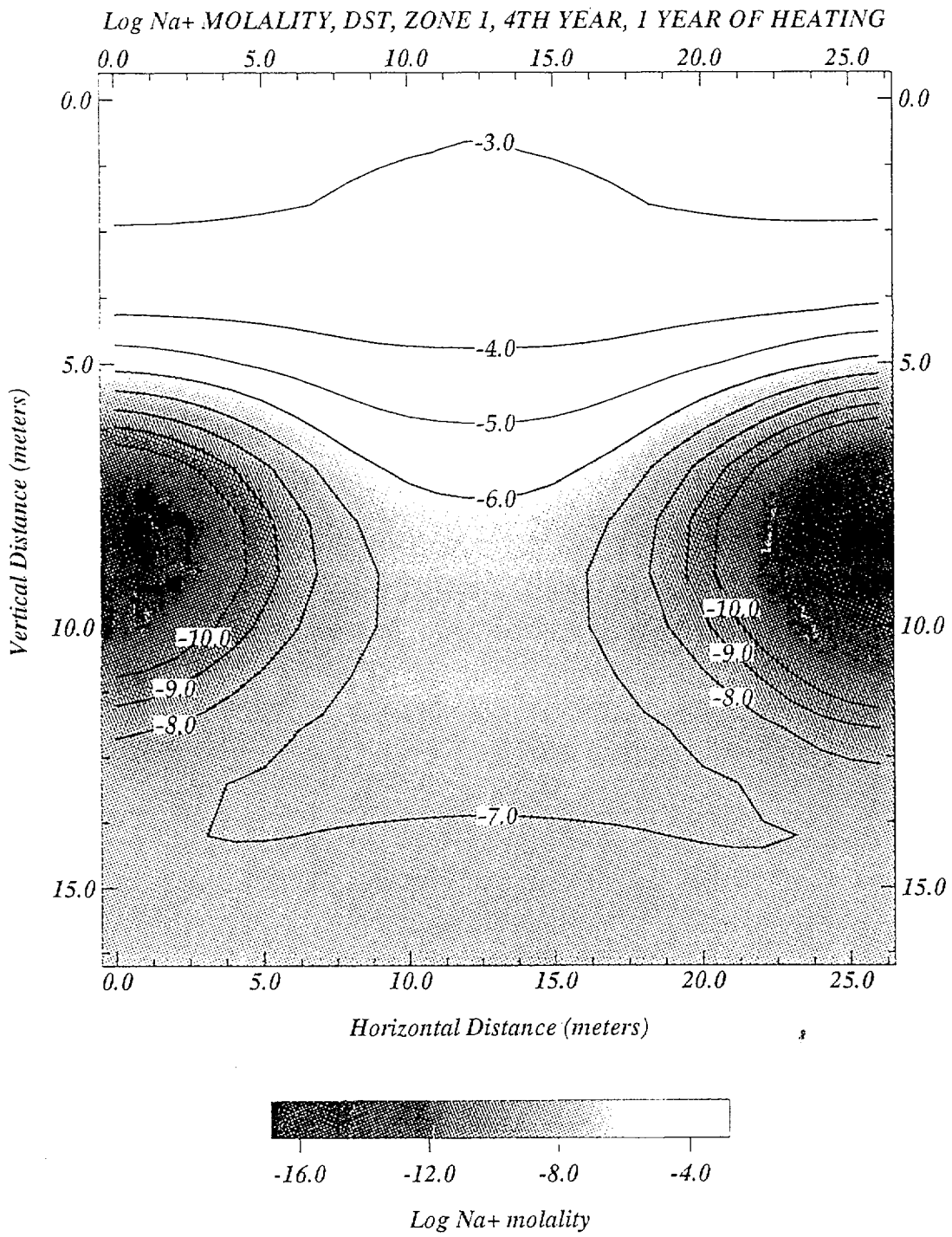
Log Na+ MOLALITY, DST, ZONE 1, 4TH YEAR, 1 YEAR OF HEATING
0.0
5.0
10.0
15.0
20.0
25.0
-3.0
-4.0
-5.0
-6.0
-7.0
-8.0
-9.0
-10.0
Vertical Distance (meters)
Horizontal Distance (meters)
-16.0
-12.0
-8.0
-4.0
Log Na+ molality

Figure 6c

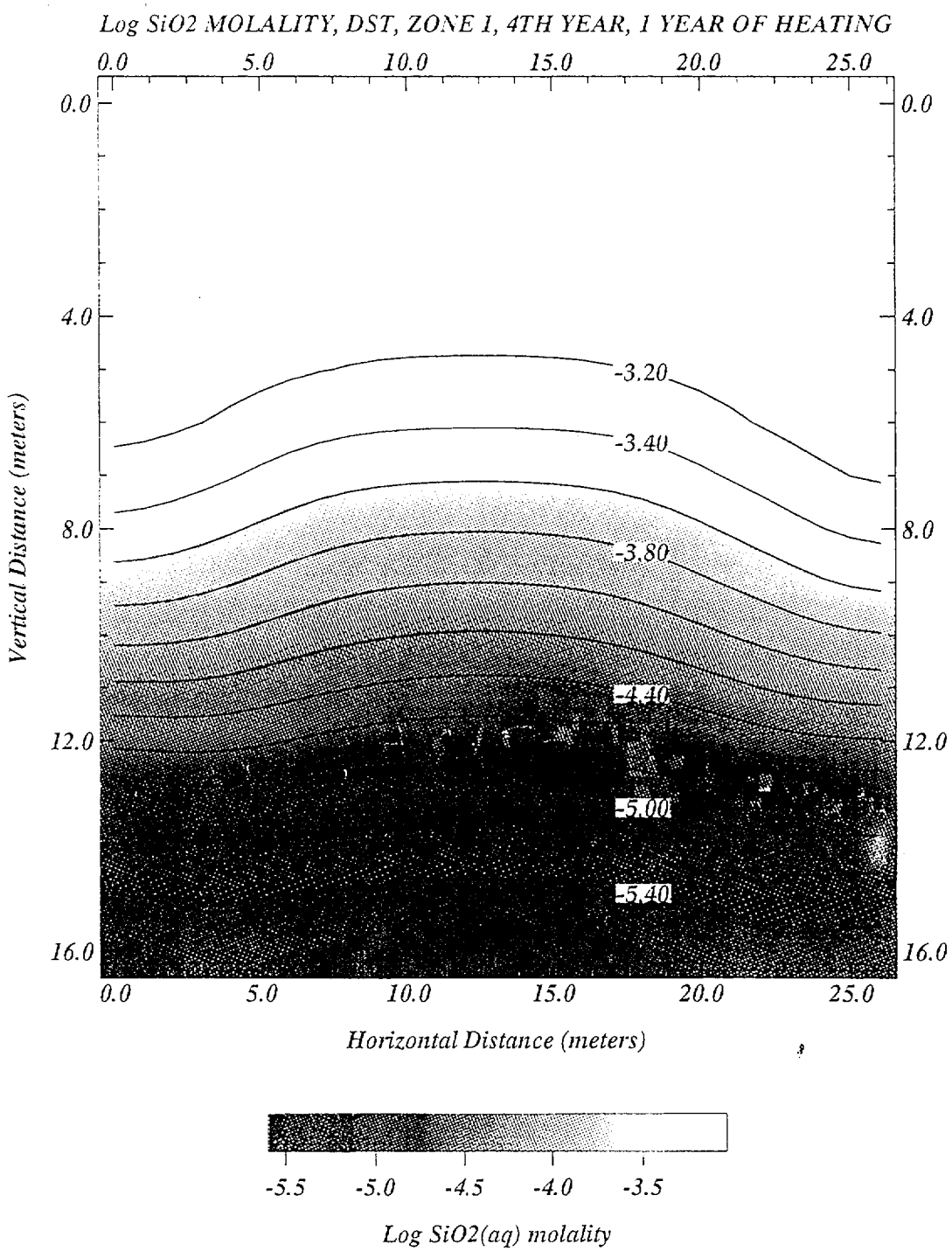
Log SiO2 MOLALITY, DST, ZONE 1, 4TH YEAR, 1 YEAR OF HEATING
0.0
5.0
10.0
15.0
20.0
25.0
4.0
8.0
12.0
16.0
-3.20
-3.40
-3.80
-4.40
-5.00
-5.40
Vertical Distance (meters)
Horizontal Distance (meters)
-5.5
-5.0
-4.5
-4.0
-3.5
Log SiO2(aq) molality

Figure 6d

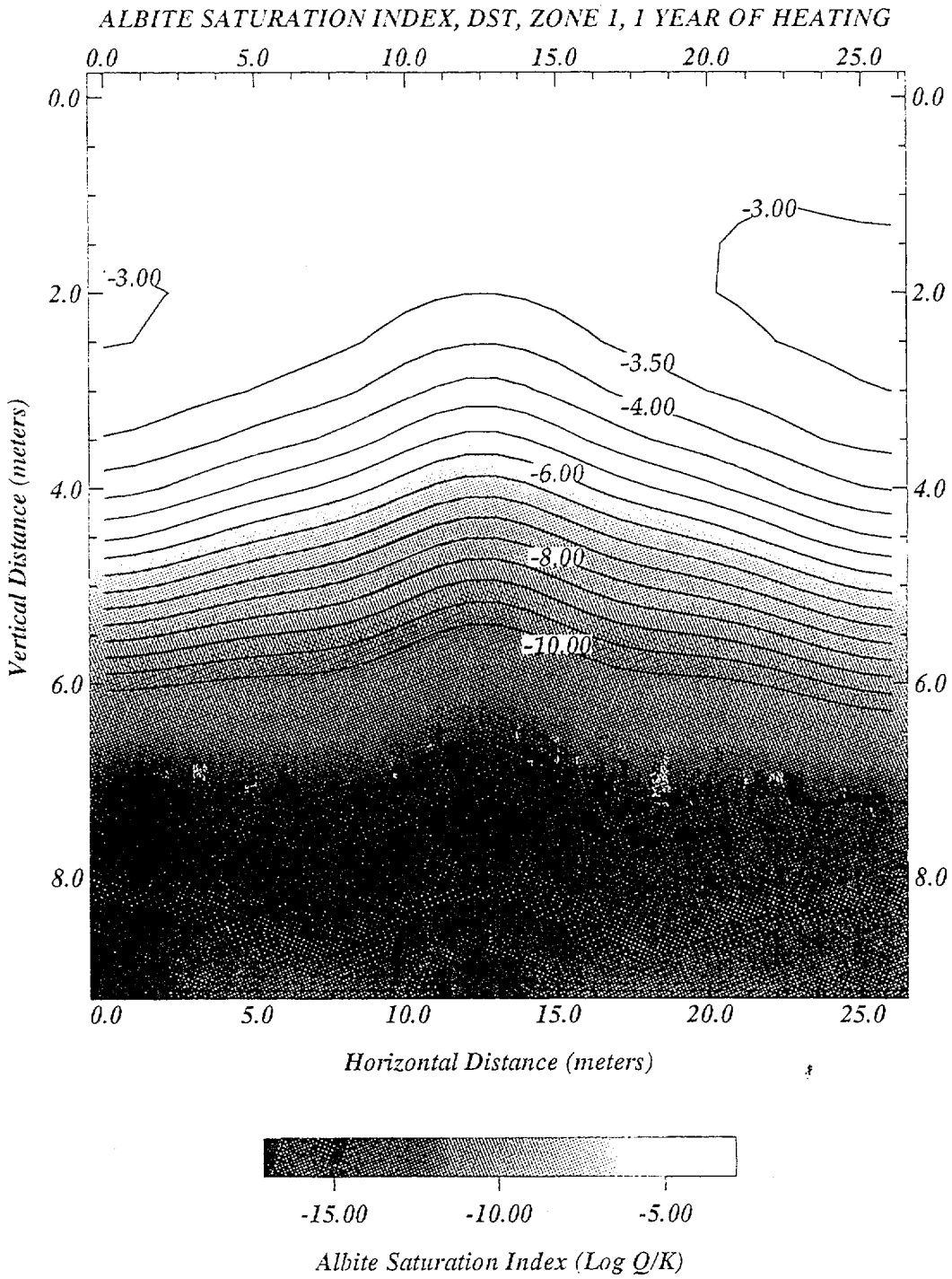
ALBITE SATURATION INDEX, DST, ZONE 1, 1 YEAR OF HEATING
0.0
5.0
10.0
15.0
20.0
25.0
0.0
2.0
4.0
6.0
8.0
-3.00
-3.00
-3.50
-4.00
-6.00
-8.00
-10.00
Vertical Distance (meters)
Horizontal Distance (meters)
-15.00
-10.00
-5.00
Albite Saturation Index (Log Q/K)

Figure 7a

CALCITE SATURATION INDEX, DST, ZONE 1, 1 YEAR OF HEATING

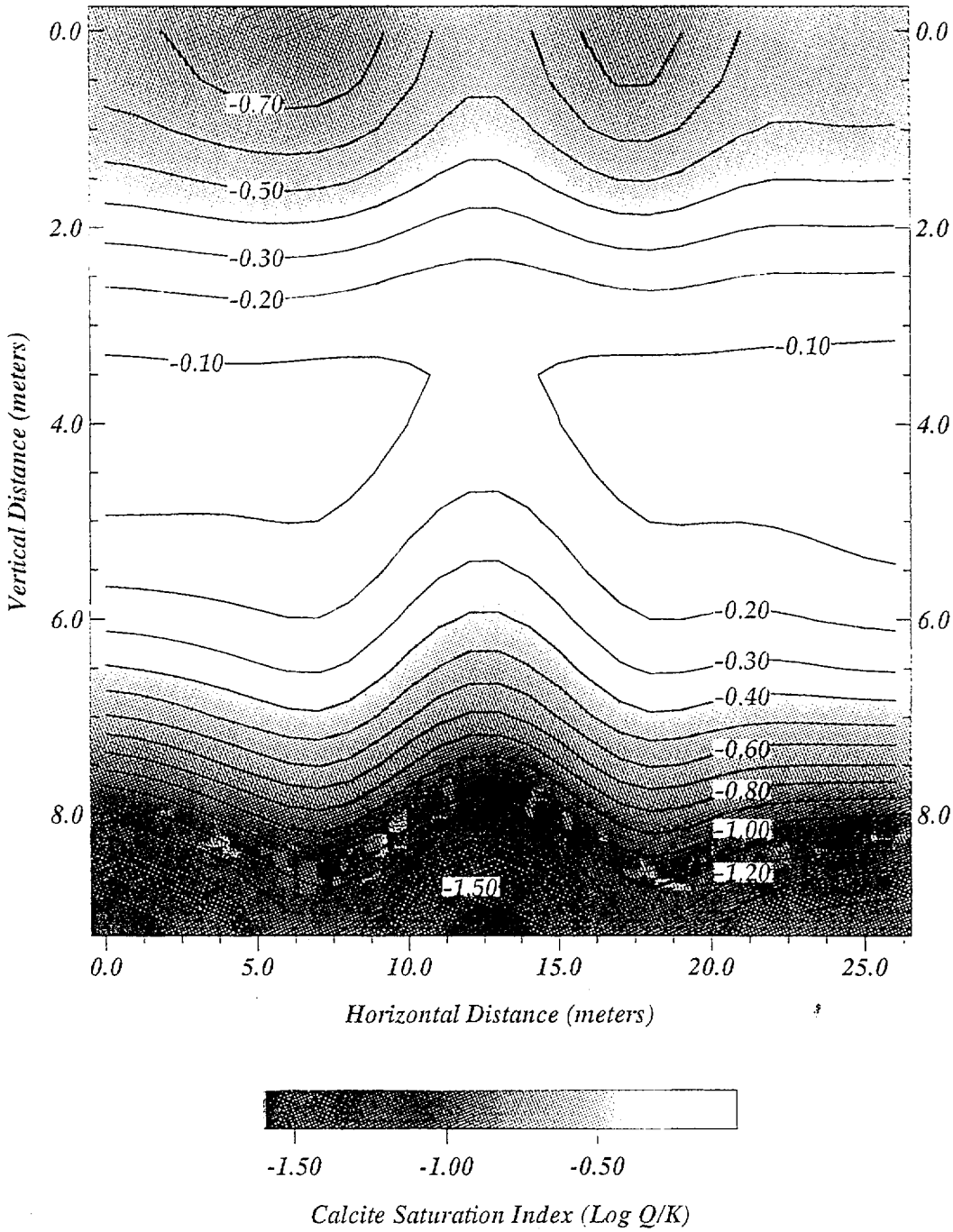

Figure 7b

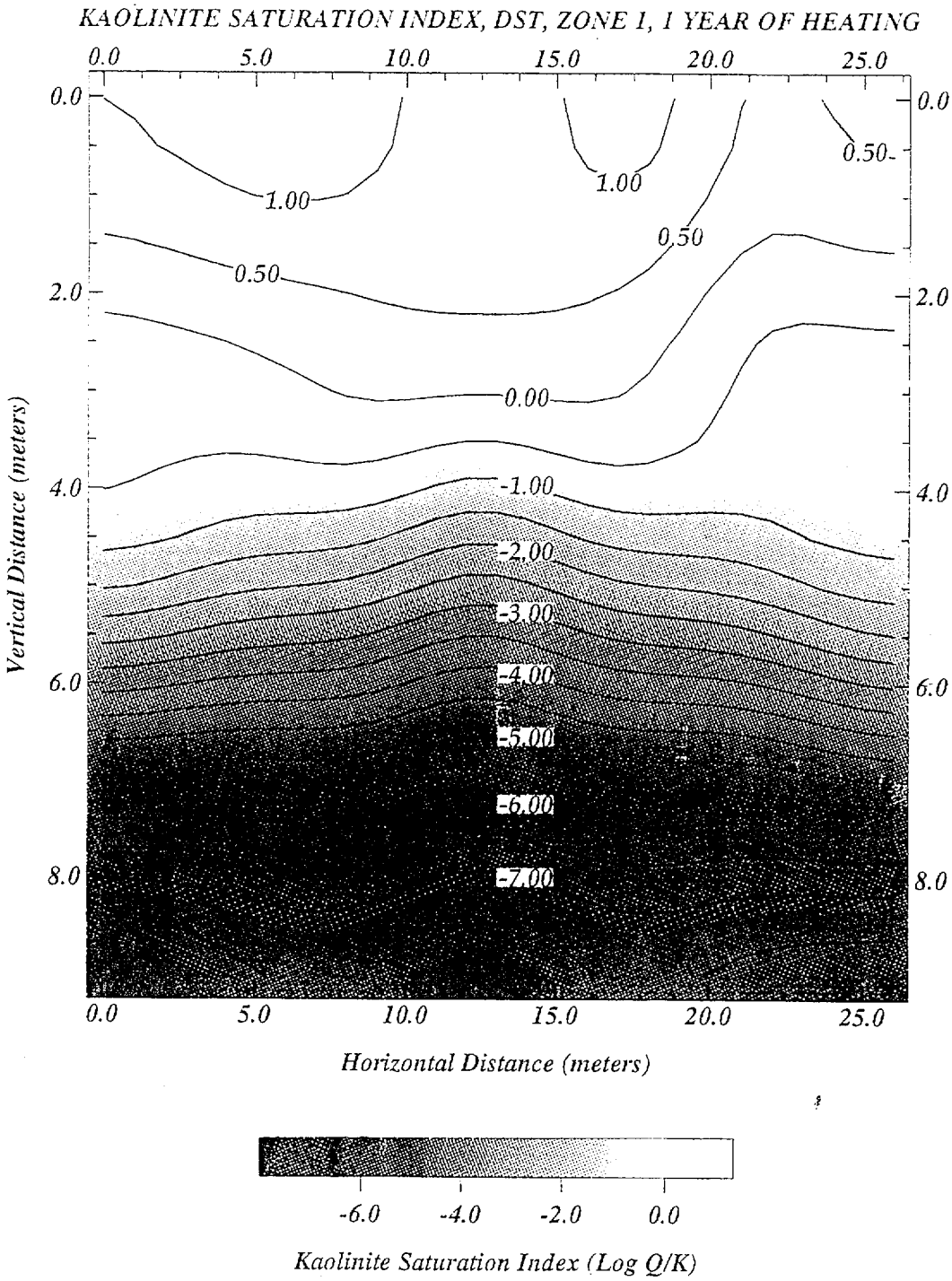
KAOLINITE SATURATION INDEX, DST, ZONE 1, 1 YEAR OF HEATING
0.0
5.0
10.0
15.0
20.0
25.0
0.0
2.0
4.0
6.0
8.0
1.00
0.50
0.00
-1.00
-2.00
-3.00
-4.00
-5.00
-6.00
-7.00
Vertical Distance (meters)
Horizontal Distance (meters)
-6.0
-4.0
-2.0
0.0
Kaolinite Saturation Index (Log Q/K)

Figure 7c

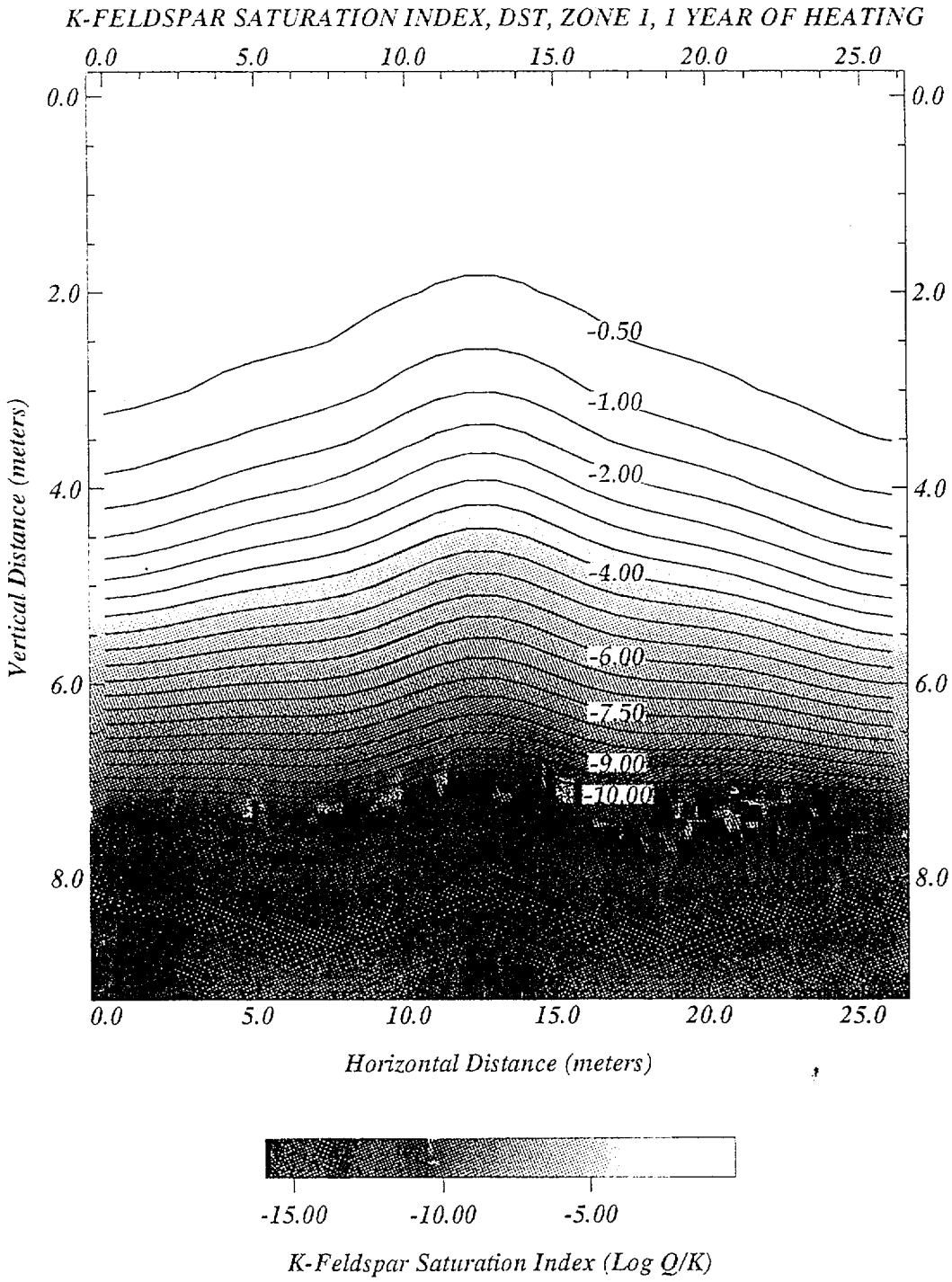
K-FELDSPAR SATURATION INDEX, DST, ZONE 1, 1 YEAR OF HEATING
0.0
5.0
10.0
15.0
20.0
25.0
2.0
4.0
6.0
8.0
Vertical Distance (meters)
-0.50
-1.00
-2.00
-4.00
-6.00
-7.50
-9.00
-10.00
Horizontal Distance (meters)
-15.00
-10.00
-5.00
K-Feldspar Saturation Index (Log Q/K)

Figure 7d

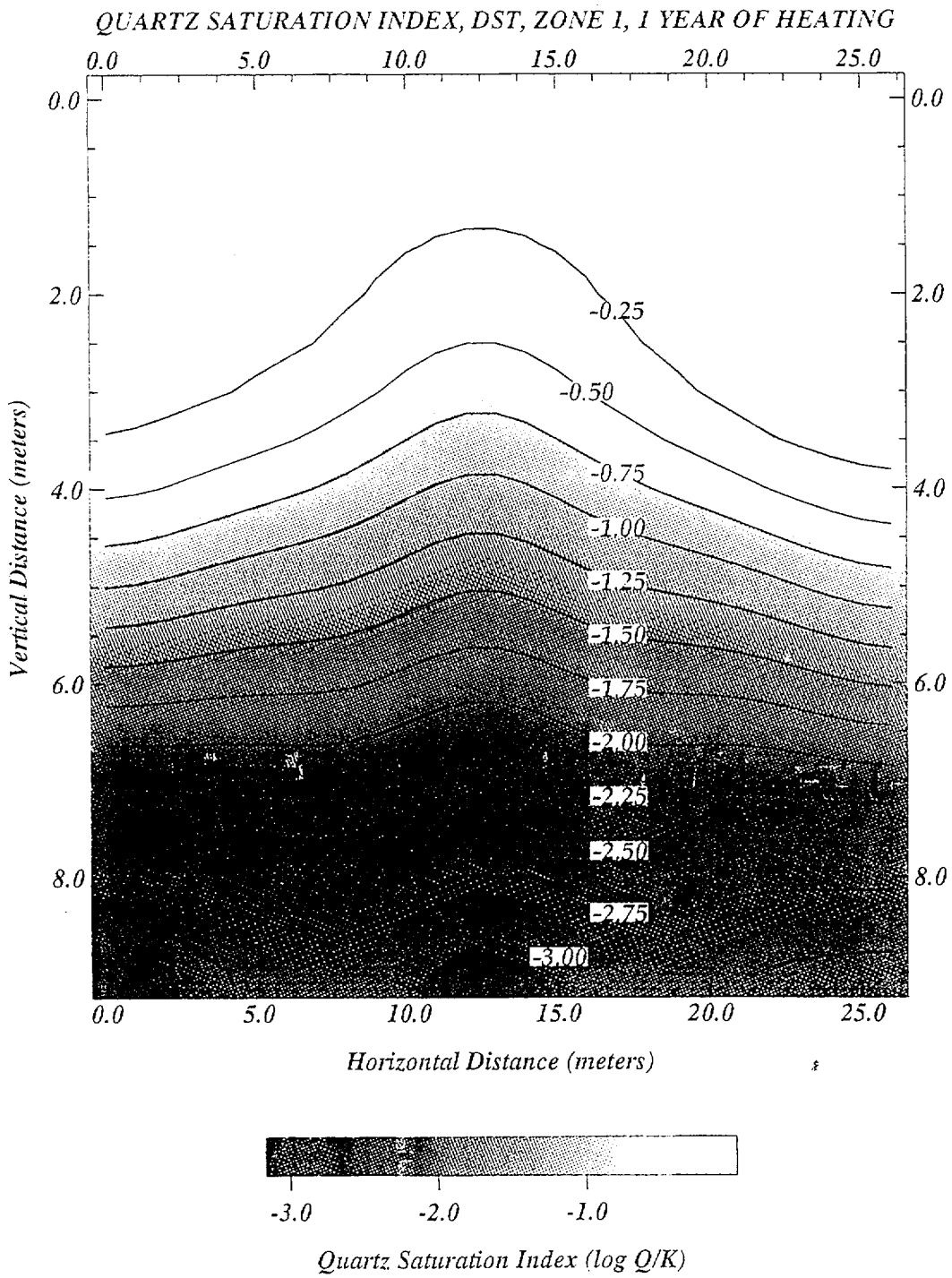
QUARTZ SATURATION INDEX, DST, ZONE 1, 1 YEAR OF HEATING
0.0
5.0
10.0
15.0
20.0
25.0
0.0
2.0
4.0
6.0
8.0
Vertical Distance (meters)
-0.25
-0.50
-0.75
-1.00
-1.25
-1.50
-1.75
-2.00
-2.25
-2.50
-2.75
-3.00
Horizontal Distance (meters)
-3.0
-2.0
-1.0
Quartz Saturation Index (log Q/K)

Figure 7e

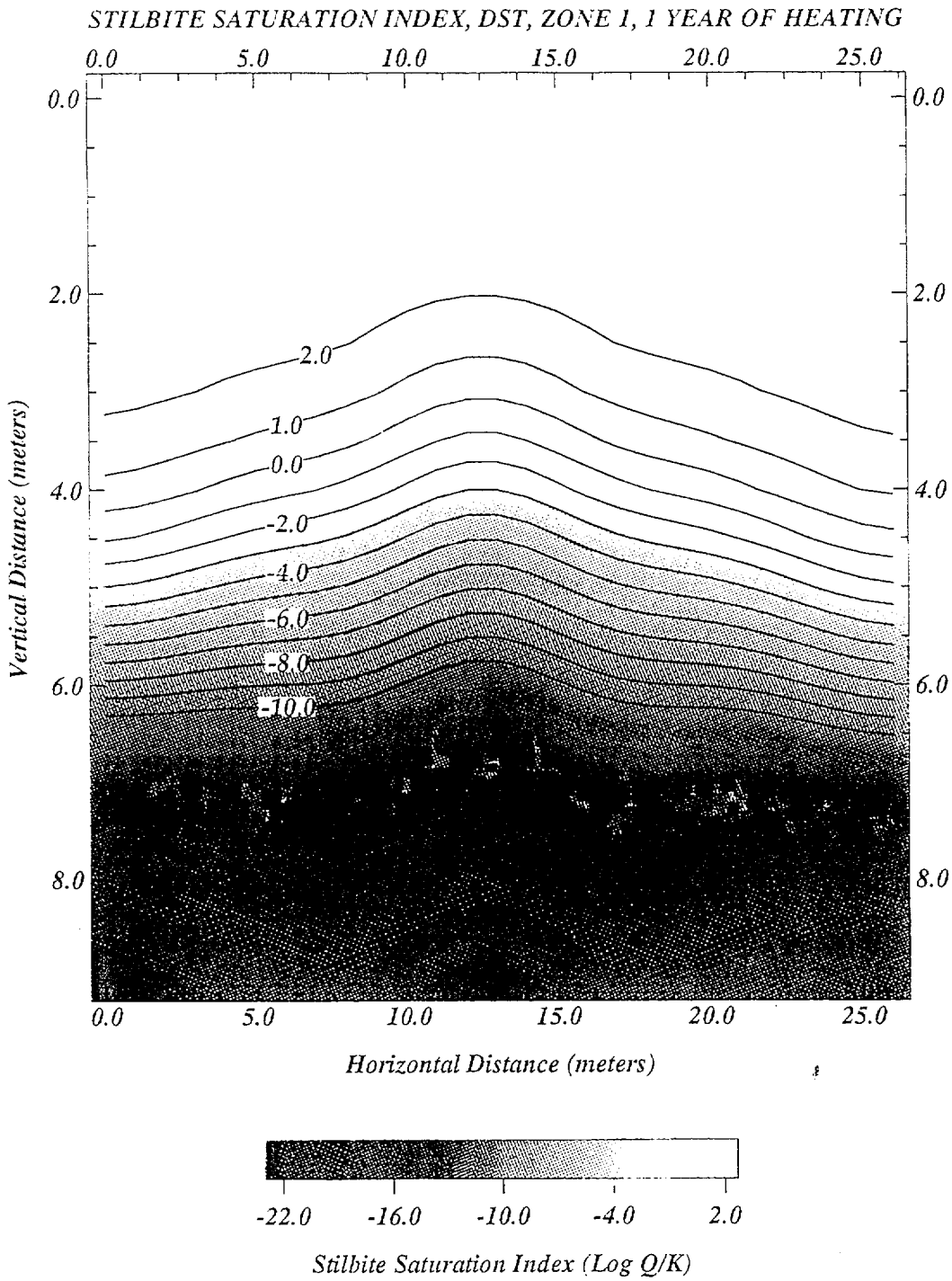
STILBITE SATURATION INDEX, DST, ZONE 1, 1 YEAR OF HEATING
0.0
5.0
10.0
15.0
20.0
25.0
0.0
2.0
4.0
6.0
8.0
Vertical Distance (meters)
2.0
1.0
0.0
-2.0
-4.0
-6.0
-8.0
-10.0
Horizontal Distance (meters)
-22.0
-16.0
-10.0
-4.0
2.0
Stilbite Saturation Index (Log Q/K)

Figure 7f

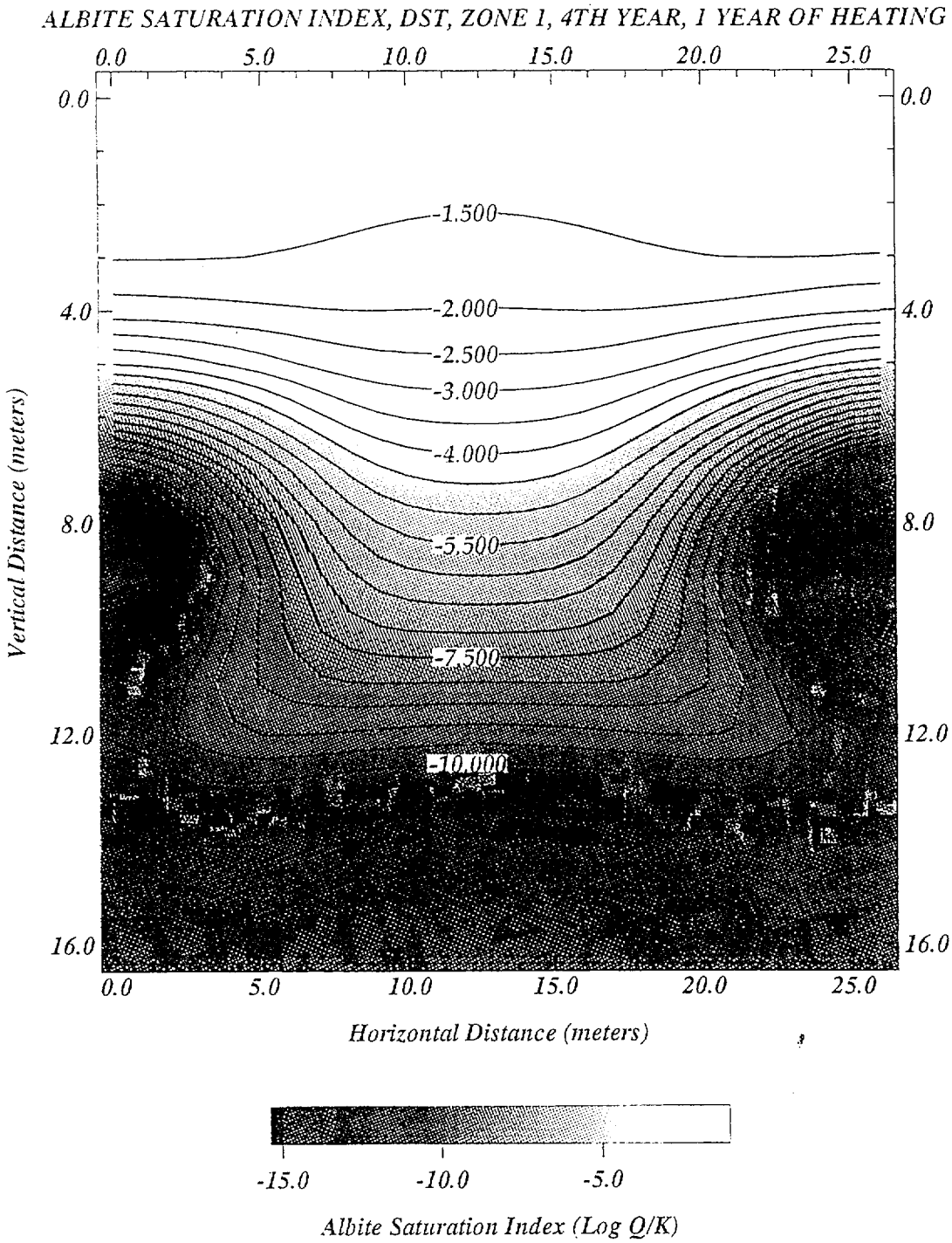
ALBITE SATURATION INDEX, DST, ZONE 1, 4TH YEAR, 1 YEAR OF HEATING
0.0
5.0
10.0
15.0
20.0
25.0
4.0
8.0
12.0
16.0
-1.500
-2.000
-2.500
-3.000
-4.000
-5.500
-7.500
-10.000
Vertical Distance (meters)
Horizontal Distance (meters)
-15.0
-10.0
-5.0
Albite Saturation Index (Log Q/K)

Figure 8a

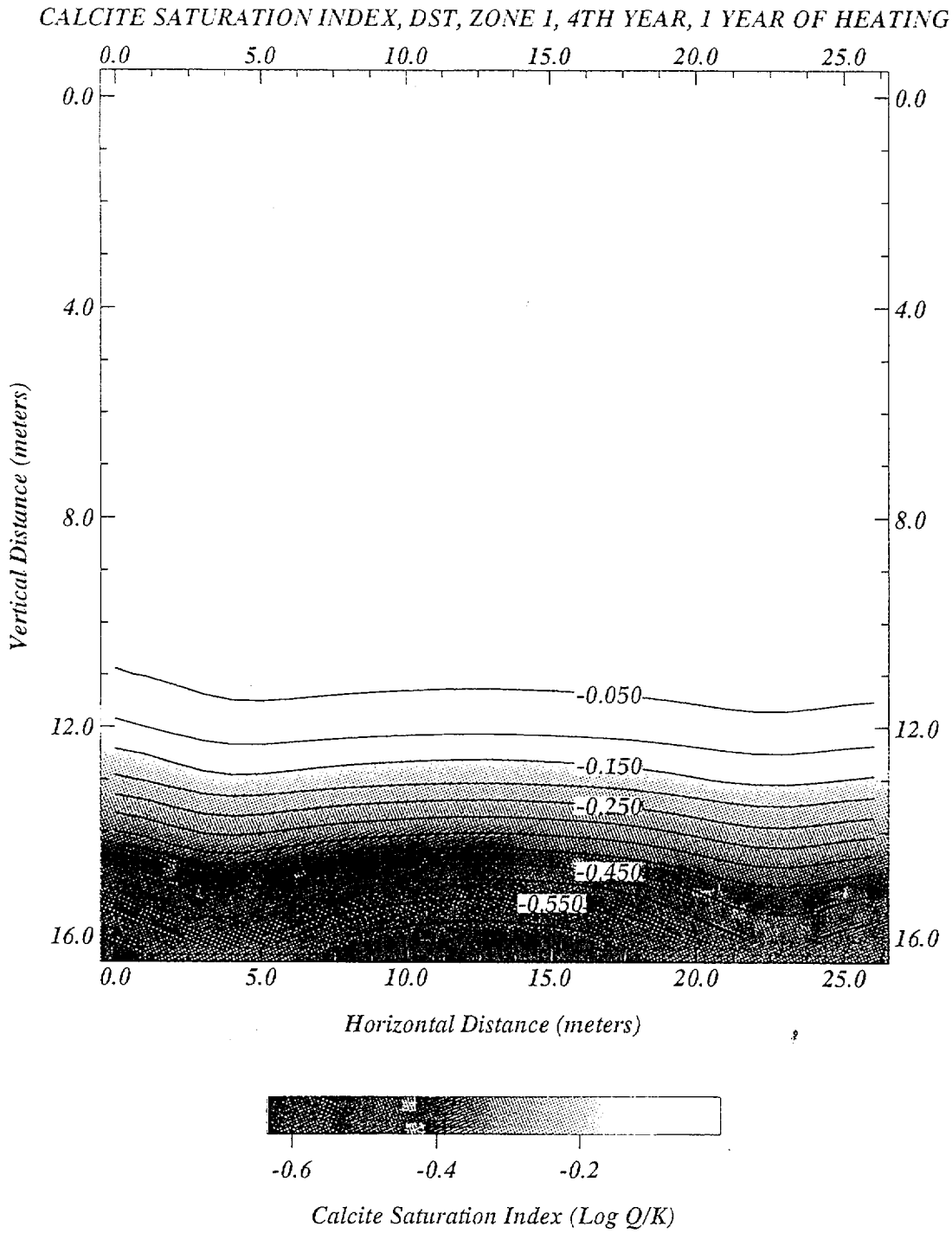
CALCITE SATURATION INDEX, DST, ZONE 1, 4TH YEAR, 1 YEAR OF HEATING
0.0
5.0
10.0
15.0
20.0
25.0
4.0
8.0
12.0
16.0
Vertical Distance (meters)
-0.050
-0.150
-0.250
-0.450
-0.550
Horizontal Distance (meters)
-0.6
-0.4
-0.2
Calcite Saturation Index (Log Q/K)

Figure 8b

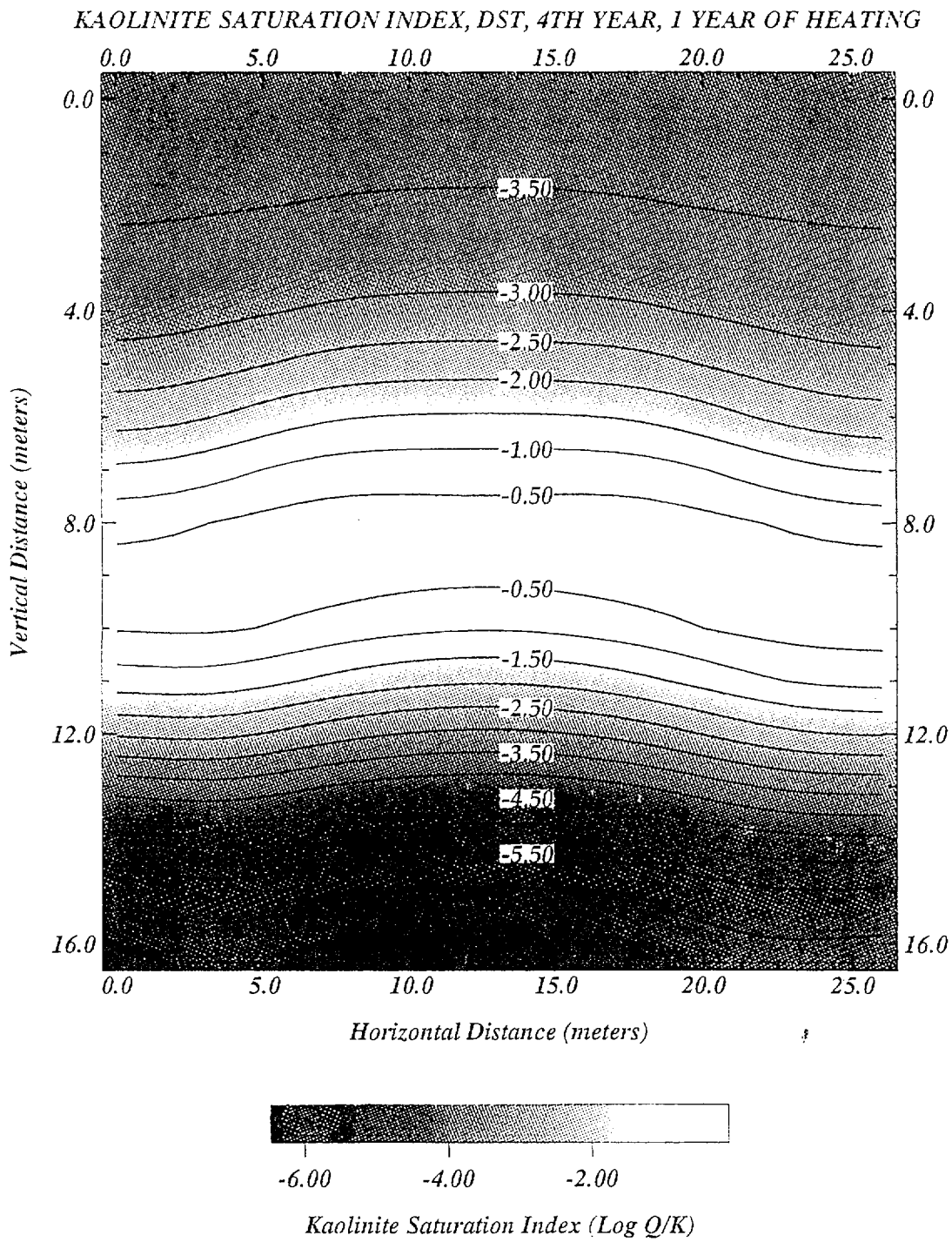
KAOLINITE SATURATION INDEX, DST, 4TH YEAR, 1 YEAR OF HEATING
0.0
5.0
10.0
15.0
20.0
25.0
4.0
8.0
12.0
16.0
Vertical Distance (meters)
-3.50
-3.00
-2.50
-2.00
-1.00
-0.50
-0.50
-1.50
-2.50
-3.50
-4.50
-5.50
Horizontal Distance (meters)
-6.00
-4.00
-2.00
Kaolinite Saturation Index (Log Q/K)

Figure 8c

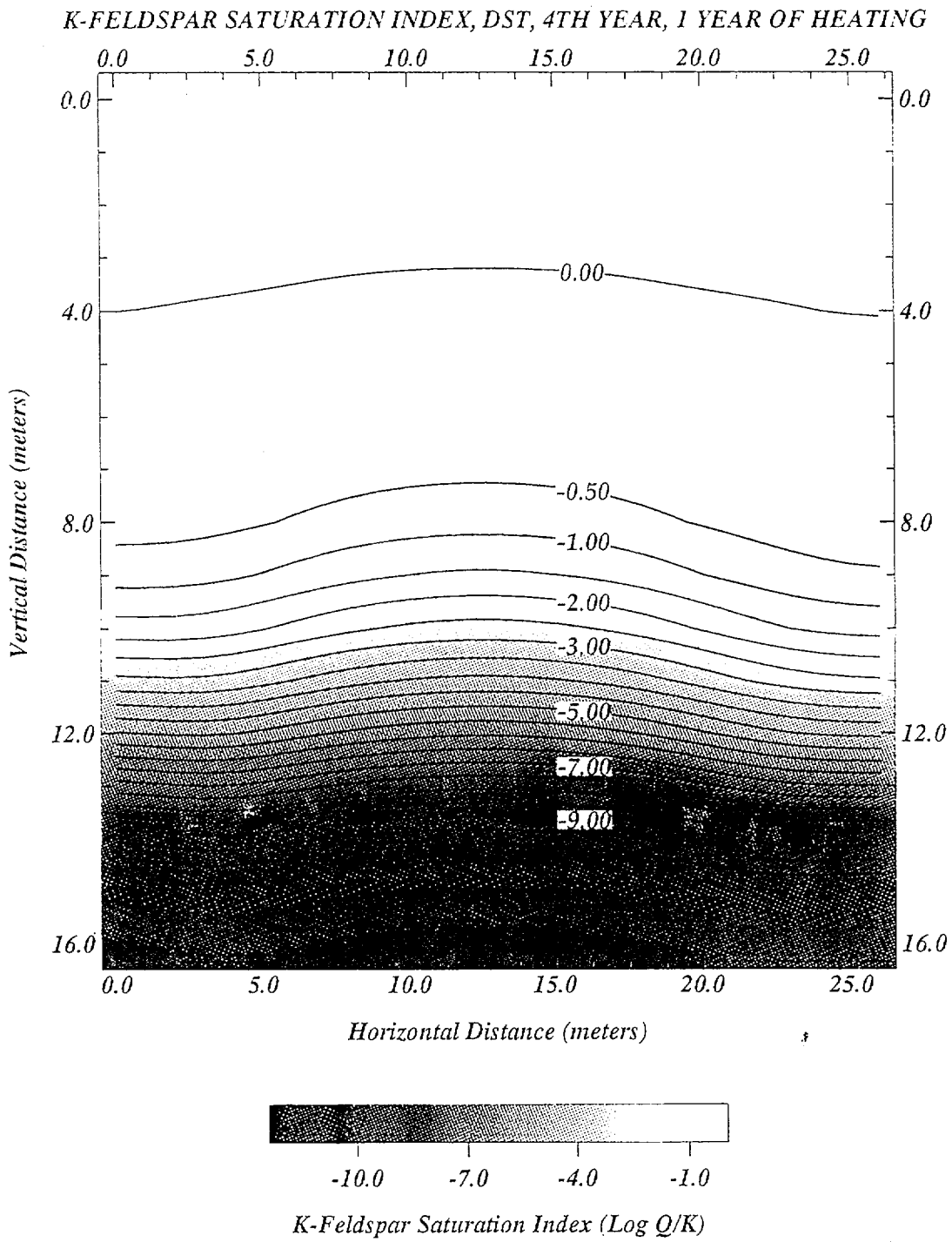
K-FELDSPAR SATURATION INDEX, DST, 4TH YEAR, 1 YEAR OF HEATING
0.0
5.0
10.0
15.0
20.0
25.0
0.0
4.0
8.0
12.0
16.0
Vertical Distance (meters)
0.00
-0.50
-1.00
-2.00
-3.00
-5.00
-7.00
-9.00
Horizontal Distance (meters)
-10.0
-7.0
-4.0
-1.0
K-Feldspar Saturation Index (Log Q/K)

Figure 8d

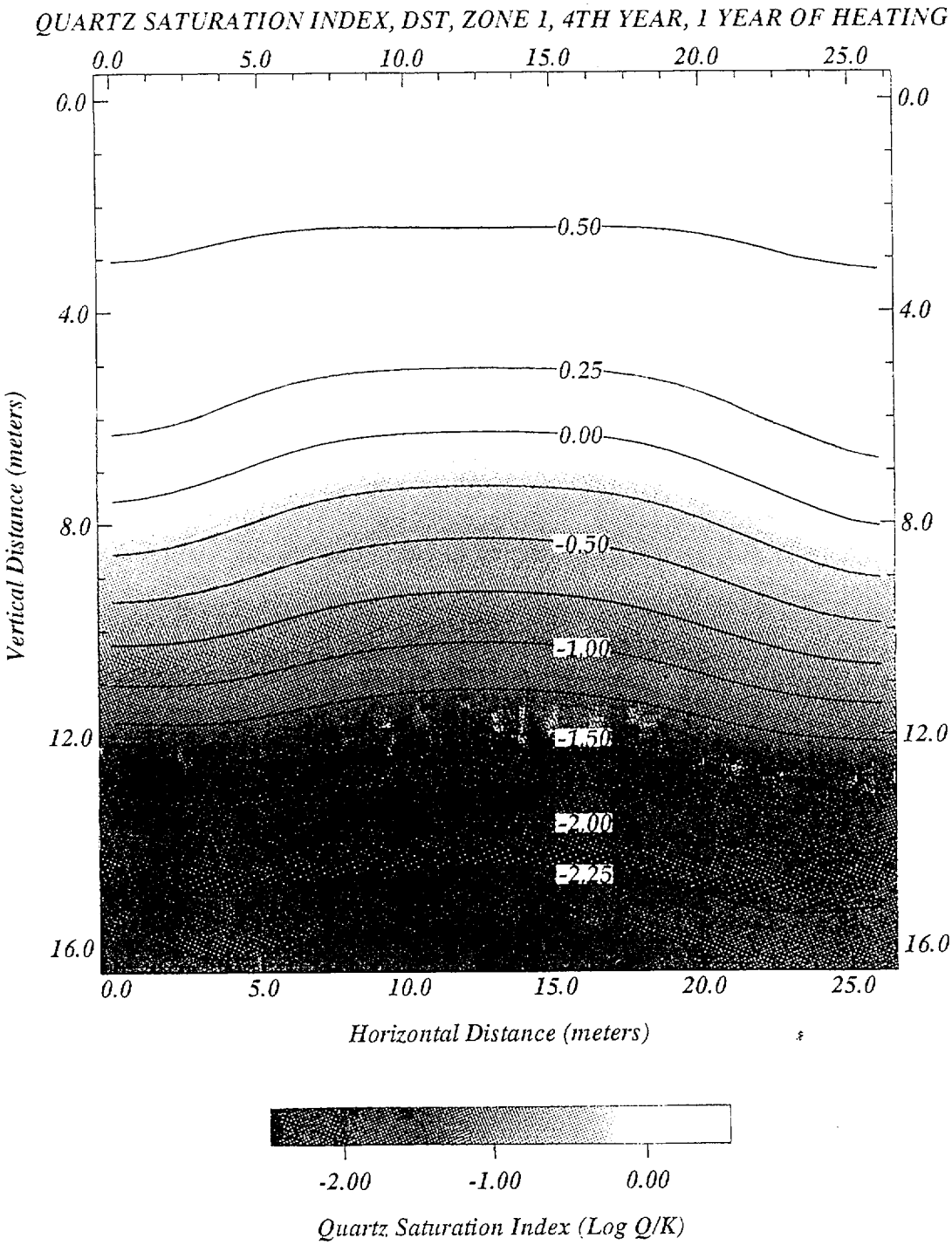
QUARTZ SATURATION INDEX, DST, ZONE 1, 4TH YEAR, 1 YEAR OF HEATING
0.0
5.0
10.0
15.0
20.0
25.0
4.0
8.0
12.0
16.0
0.50
0.25
0.00
-0.50
-1.00
-1.50
-2.00
-2.25
Vertical Distance (meters)
Horizontal Distance (meters)
-2.00
-1.00
0.00
Quartz Saturation Index (Log Q/K)

Figure 8e

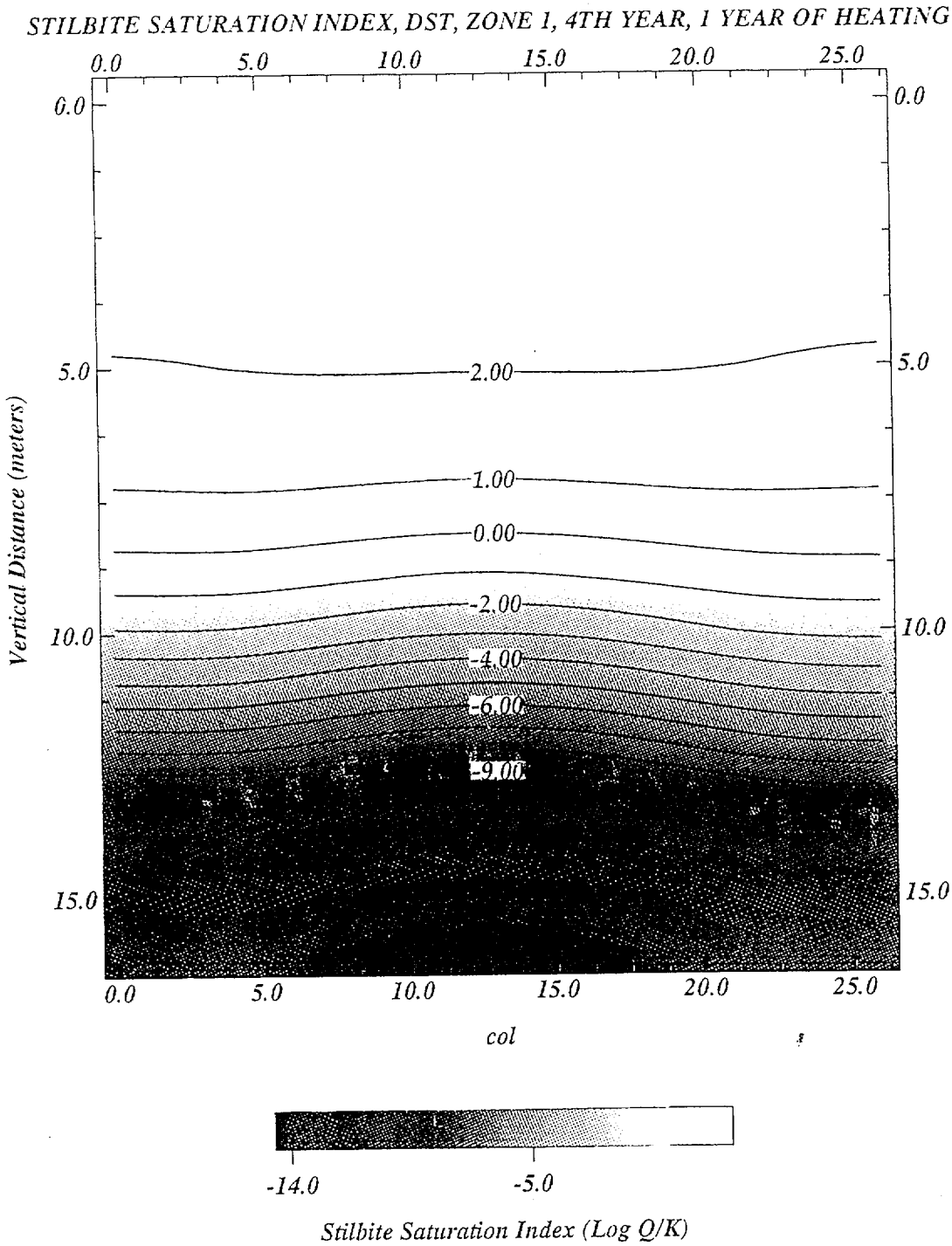
STILBITE SATURATION INDEX, DST, ZONE 1, 4TH YEAR, 1 YEAR OF HEATING
0.0
5.0
10.0
15.0
20.0
25.0
Vertical Distance (meters)
2.00
1.00
0.00
-2.00
-4.00
-6.00
-9.00
col
-14.0
-5.0
Stilbite Saturation Index (Log Q/K)

Figure 8f

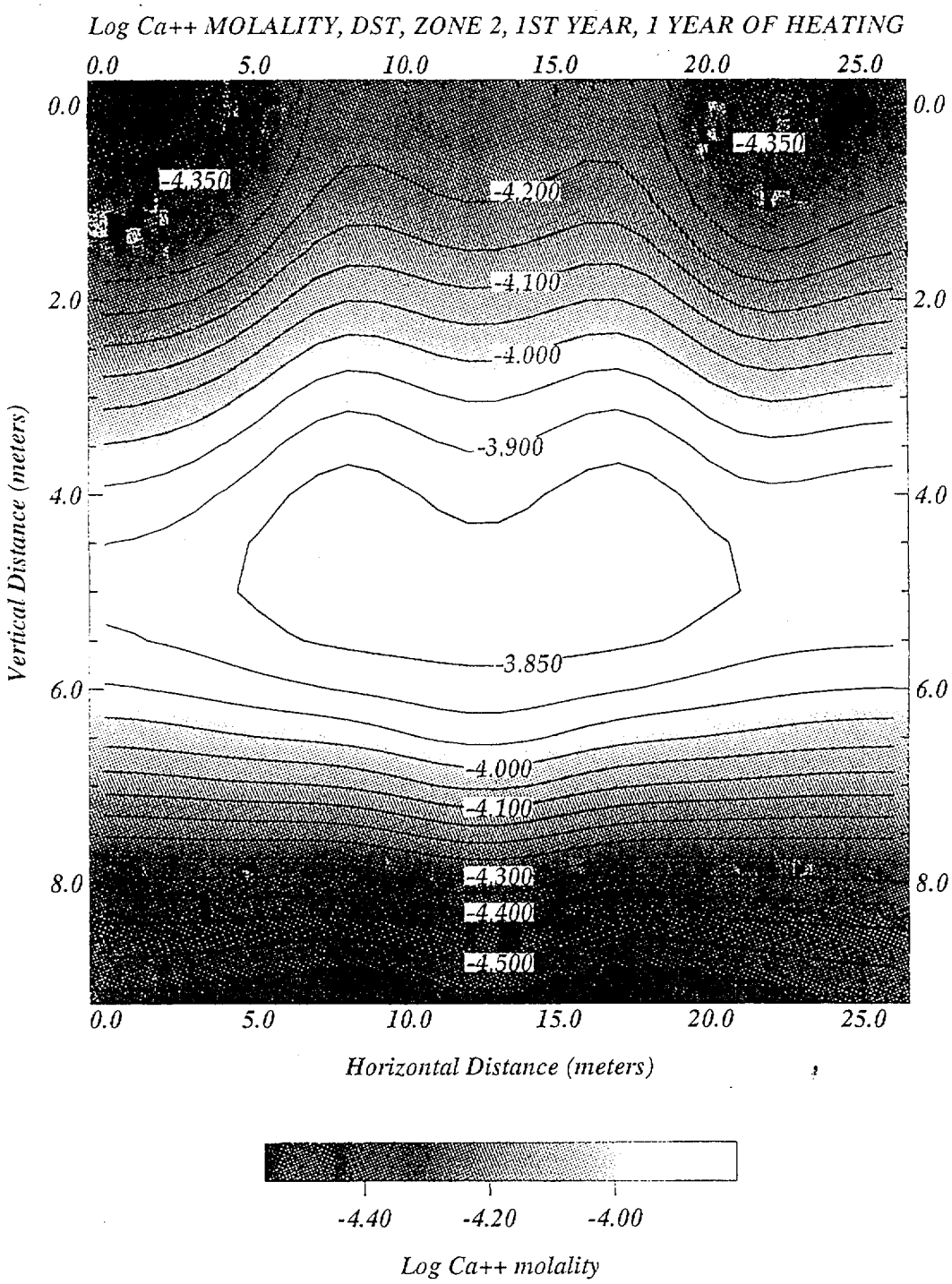
Log Ca++ MOLALITY, DST, ZONE 2, 1ST YEAR, 1 YEAR OF HEATING
0.0
5.0
10.0
15.0
20.0
25.0
0.0
2.0
4.0
6.0
8.0
Vertical Distance (meters)
-4.350
-4.350
-4.200
-4.100
-4.000
-3.900
-3.850
-4.000
-4.100
-4.300
-4.400
-4.500
Horizontal Distance (meters)
-4.40
-4.20
-4.00
Log Ca++ molality

Figure 9a

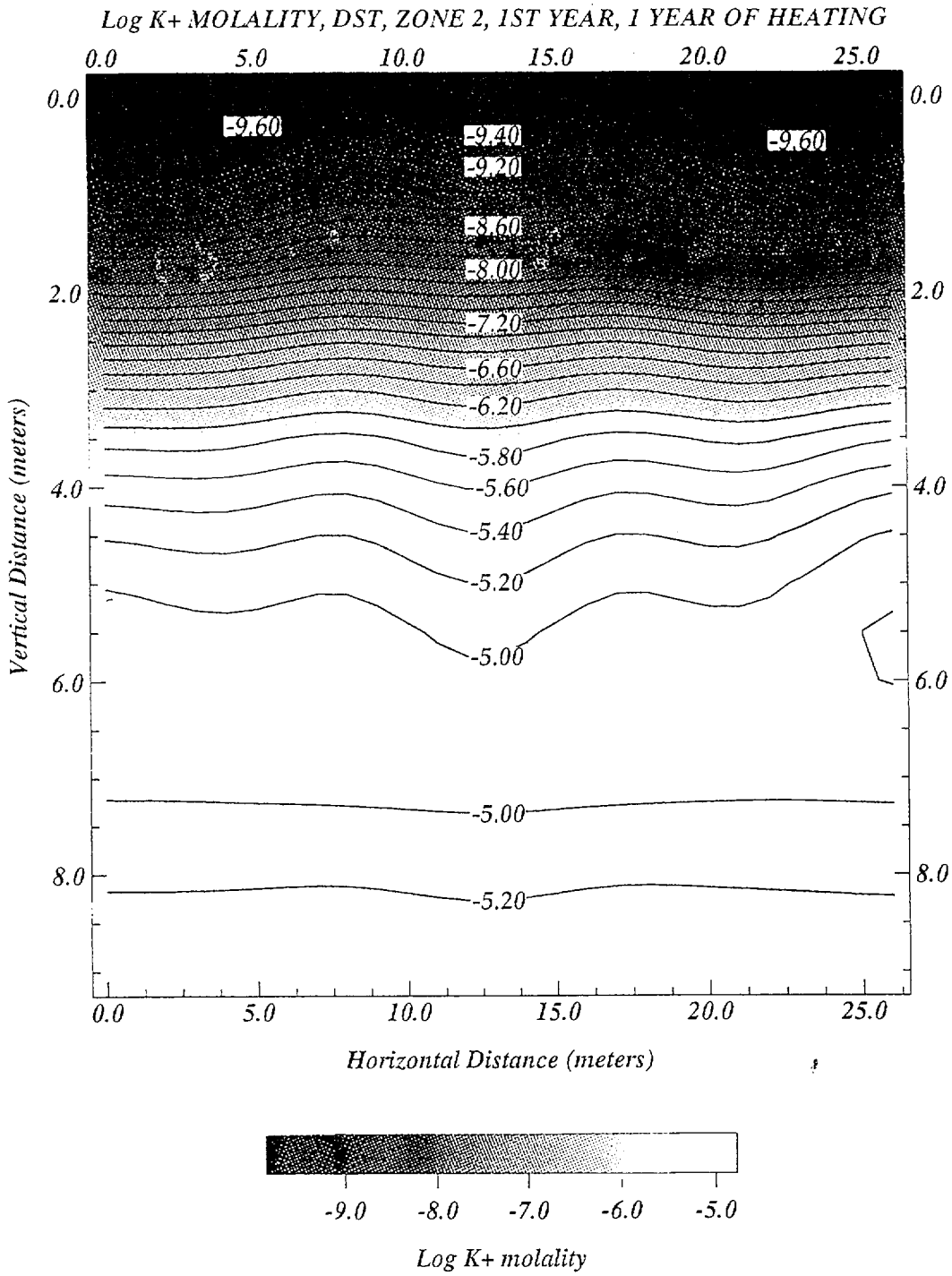
Log K+ MOLALITY, DST, ZONE 2, 1ST YEAR, 1 YEAR OF HEATING
0.0
5.0
10.0
15.0
20.0
25.0
2.0
4.0
6.0
8.0
Vertical Distance (meters)
Horizontal Distance (meters)
-9.60
-9.40
-9.20
-8.60
-8.00
-7.20
-6.60
-6.20
-5.80
-5.60
-5.40
-5.20
-5.00
-5.00
-5.20
-9.0
-8.0
-7.0
-6.0
-5.0
Log K+ molality

Figure 9b

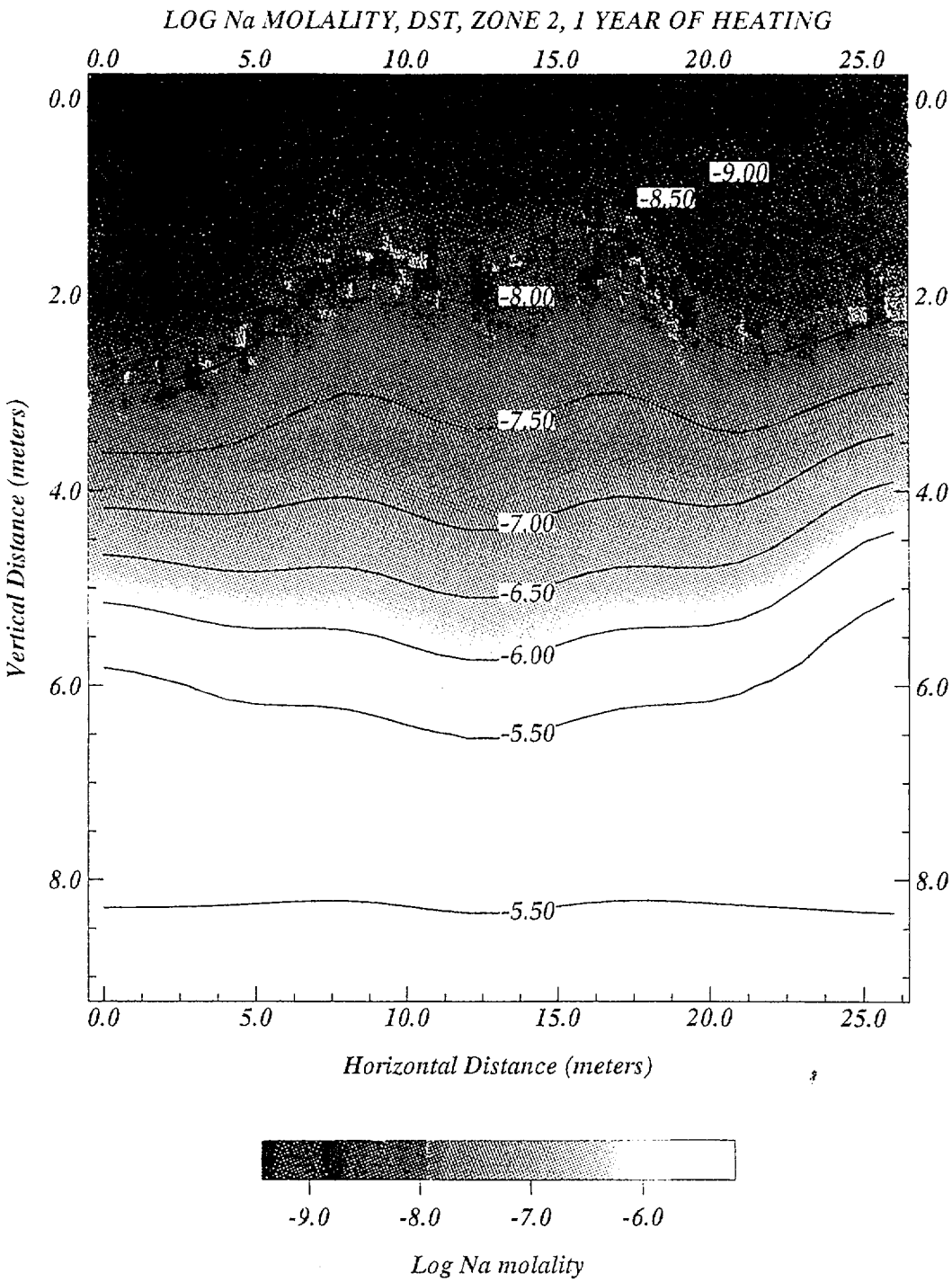
LOG Na MOLALITY, DST, ZONE 2, 1 YEAR OF HEATING
0.0
5.0
10.0
15.0
20.0
25.0
0.0
2.0
4.0
6.0
8.0
Vertical Distance (meters)
-9.00
-8.50
-8.00
-7.50
-7.00
-6.50
-6.00
-5.50
-5.50
Horizontal Distance (meters)
-9.0
-8.0
-7.0
-6.0
Log Na molality

Figure 9c

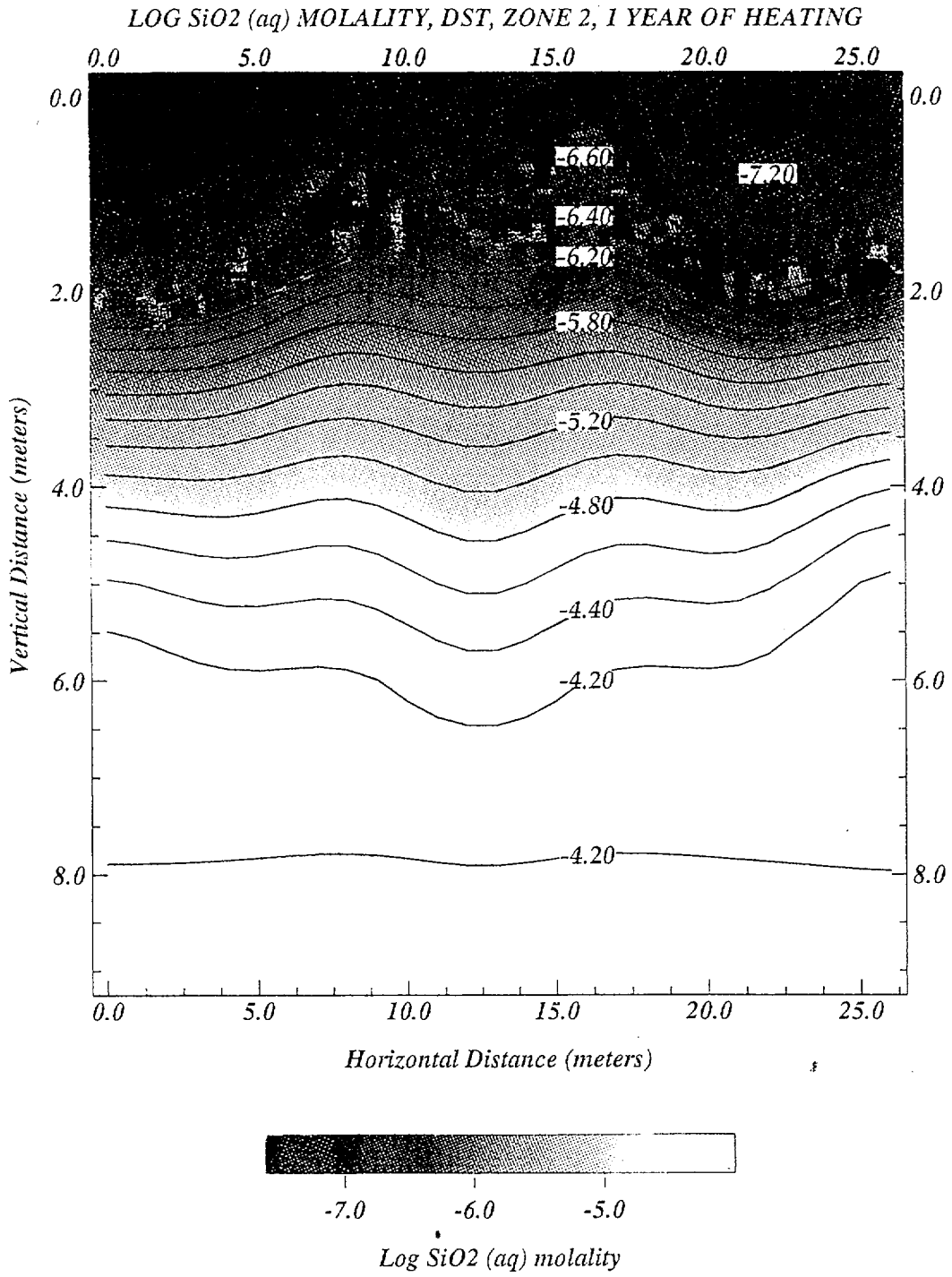
LOG SiO2 (aq) MOLALITY, DST, ZONE 2, 1 YEAR OF HEATING
0.0
5.0
10.0
15.0
20.0
25.0
0.0
2.0
4.0
6.0
8.0
-6.60
-7.20
-6.40
-6.20
-5.80
-5.20
-4.80
-4.40
-4.20
-4.20
Vertical Distance (meters)
Horizontal Distance (meters)
-7.0
-6.0
-5.0
Log SiO2 (aq) molality

Figure 9d

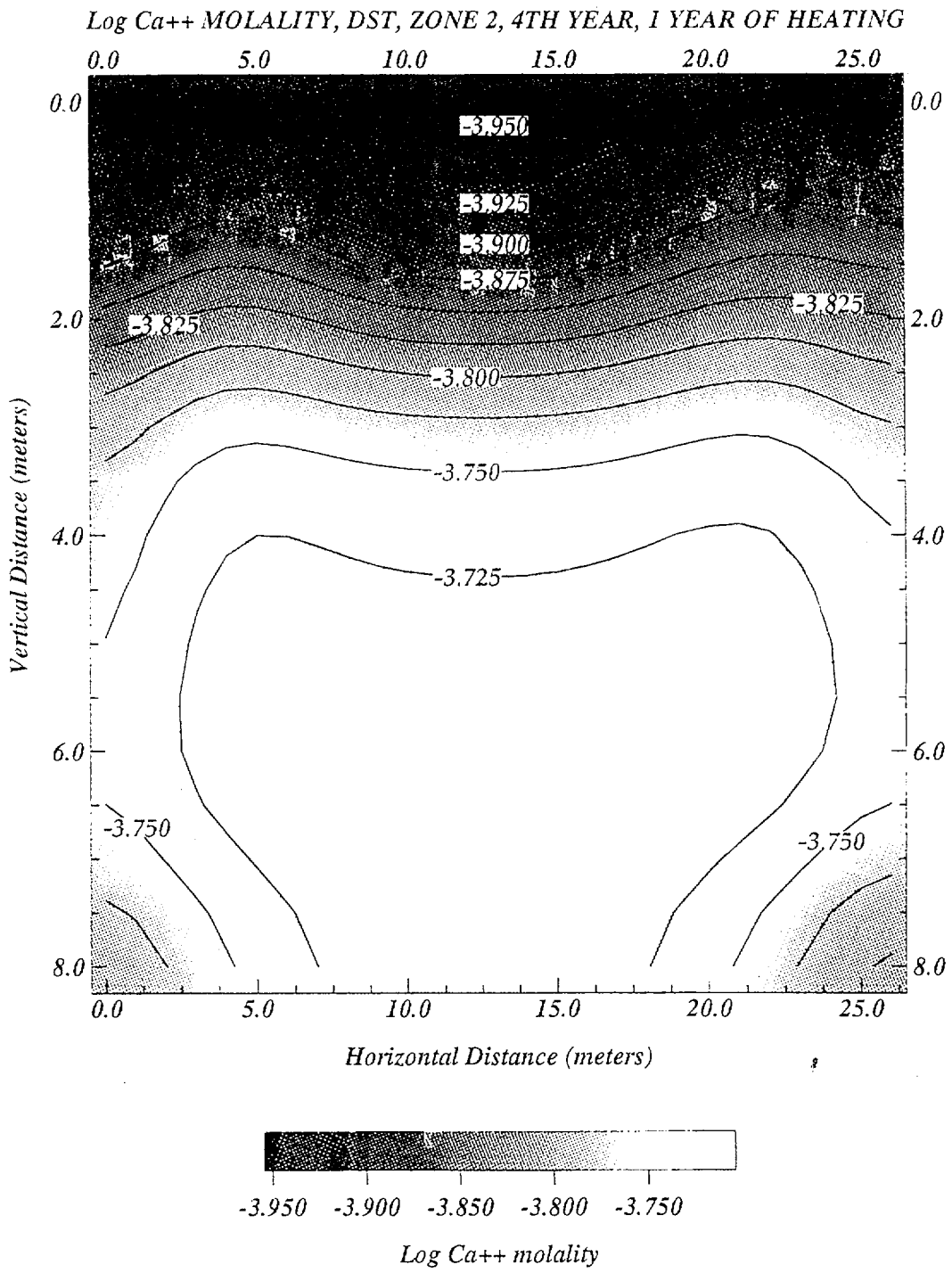
Log Ca++ MOLALITY, DST, ZONE 2, 4TH YEAR, 1 YEAR OF HEATING
0.0
5.0
10.0
15.0
20.0
25.0
2.0
4.0
6.0
8.0
-3.950
-3.925
-3.900
-3.875
-3.825
-3.800
-3.750
-3.725
Vertical Distance (meters)
Horizontal Distance (meters)
-3.950
-3.900
-3.850
-3.800
-3.750
Log Ca++ molality

Figure 10a

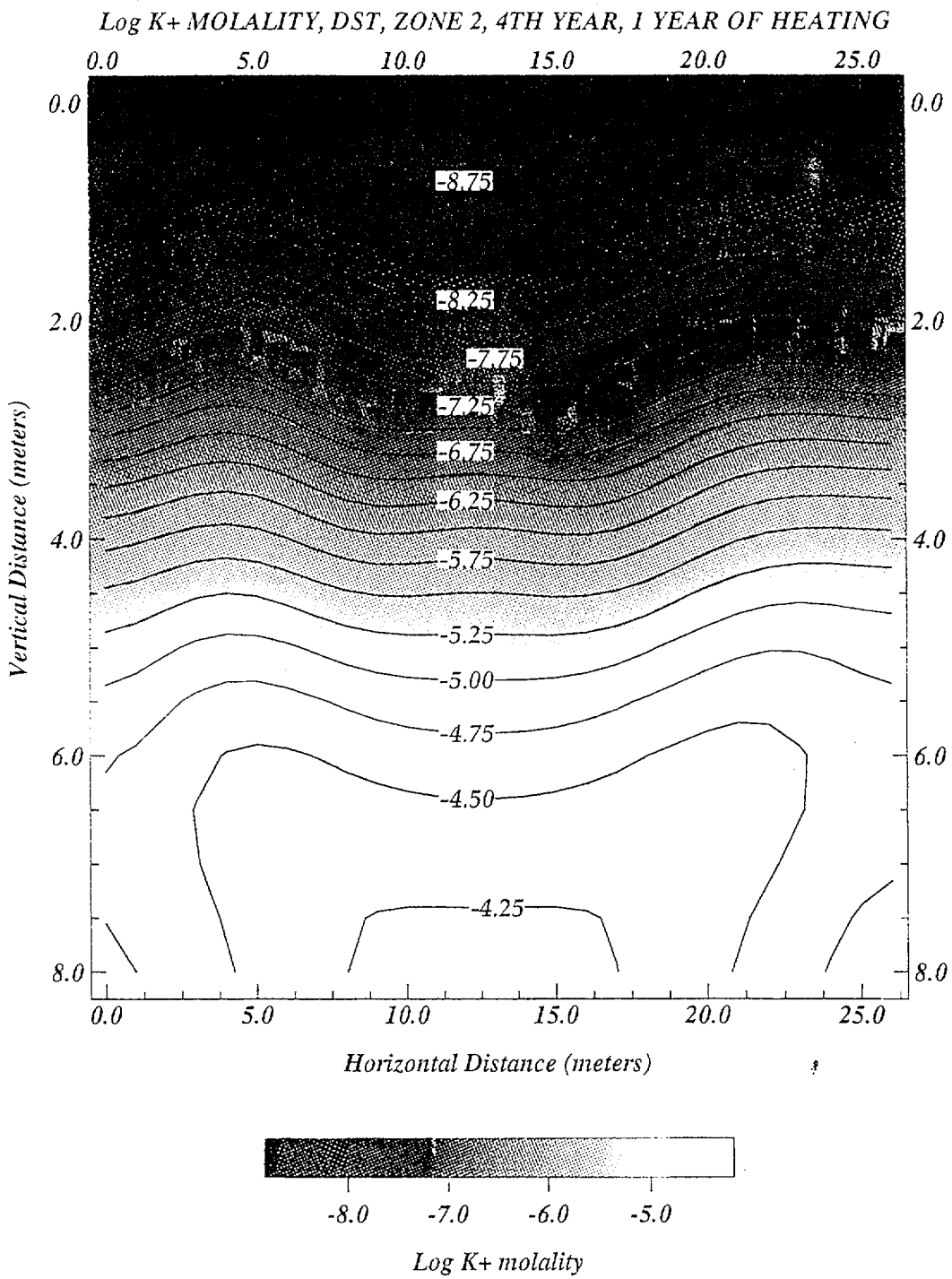
Log K+ MOLALITY, DST, ZONE 2, 4TH YEAR, 1 YEAR OF HEATING
0.0
5.0
10.0
15.0
20.0
25.0
0.0
2.0
4.0
6.0
8.0
Vertical Distance (meters)
-8.75
-8.25
-7.75
-7.25
-6.75
-6.25
-5.75
-5.25
-5.00
-4.75
-4.50
-4.25
Horizontal Distance (meters)
-8.0
-7.0
-6.0
-5.0
Log K+ molality

Figure 10b

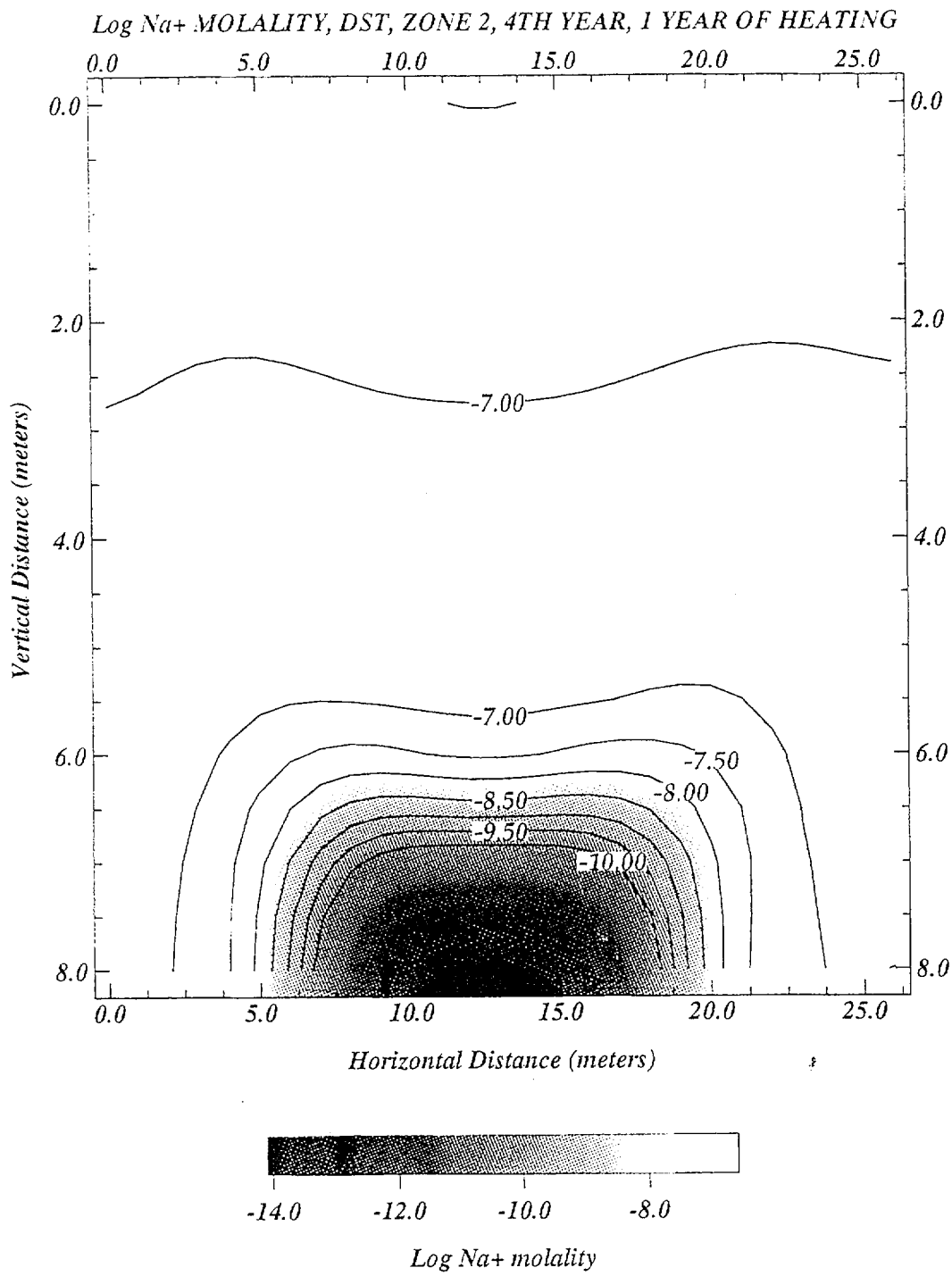
Log Na+ MOLALITY, DST, ZONE 2, 4TH YEAR, 1 YEAR OF HEATING
0.0
5.0
10.0
15.0
20.0
25.0
0.0
2.0
4.0
6.0
8.0
Vertical Distance (meters)
-7.00
-7.00
-7.50
-8.00
-8.50
-9.50
-10.00
Horizontal Distance (meters)
-14.0
-12.0
-10.0
-8.0
Log Na+ molality

Figure 10c

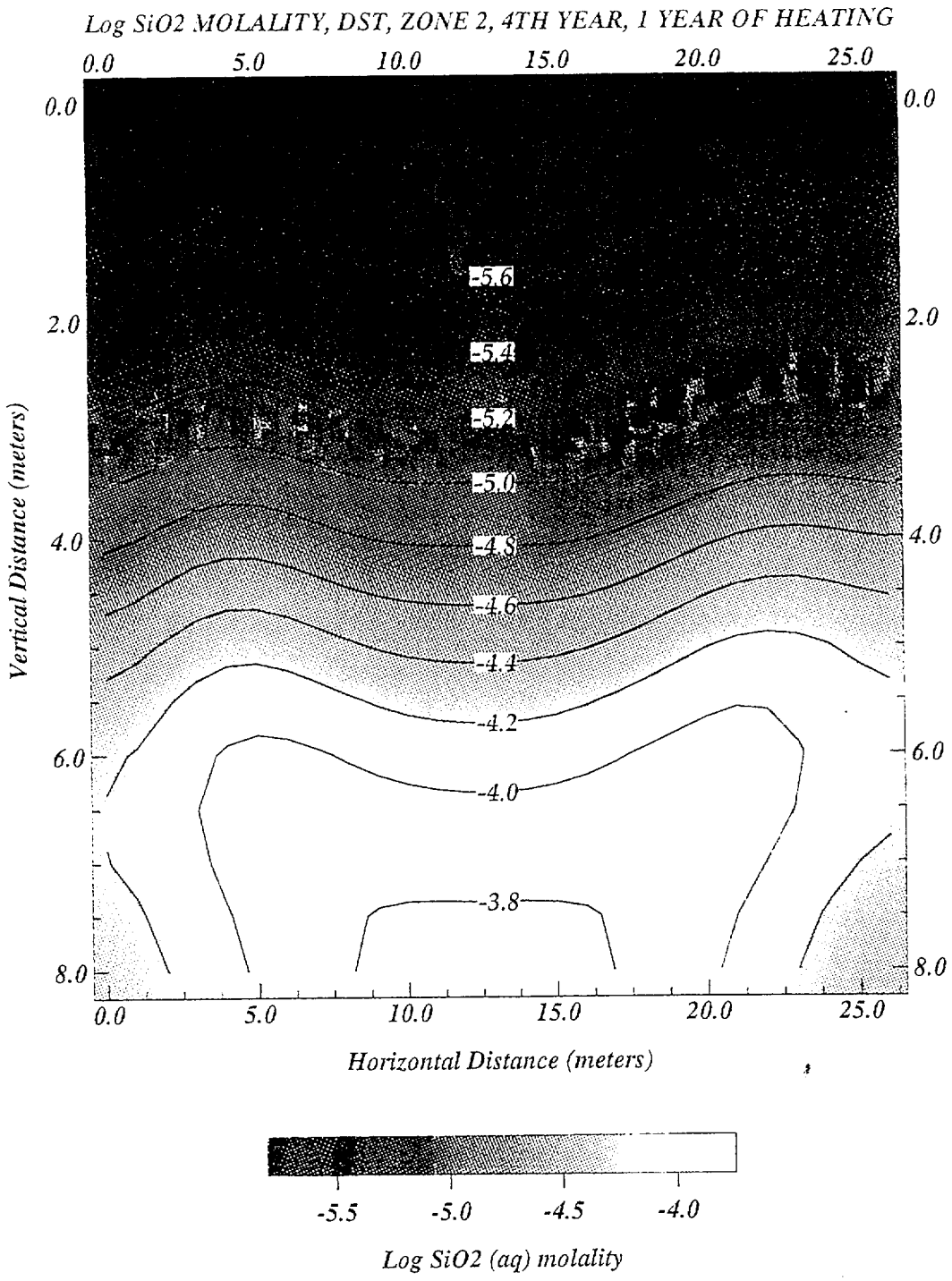
Log SiO2 MOLALITY, DST, ZONE 2, 4TH YEAR, 1 YEAR OF HEATING
0.0
5.0
10.0
15.0
20.0
25.0
0.0
2.0
4.0
6.0
8.0
Vertical Distance (meters)
-5.6
-5.4
-5.2
-5.0
-4.8
-4.6
-4.4
-4.2
-4.0
-3.8
Horizontal Distance (meters)
-5.5
-5.0
-4.5
-4.0
Log SiO2 (aq) molality

Figure 10d

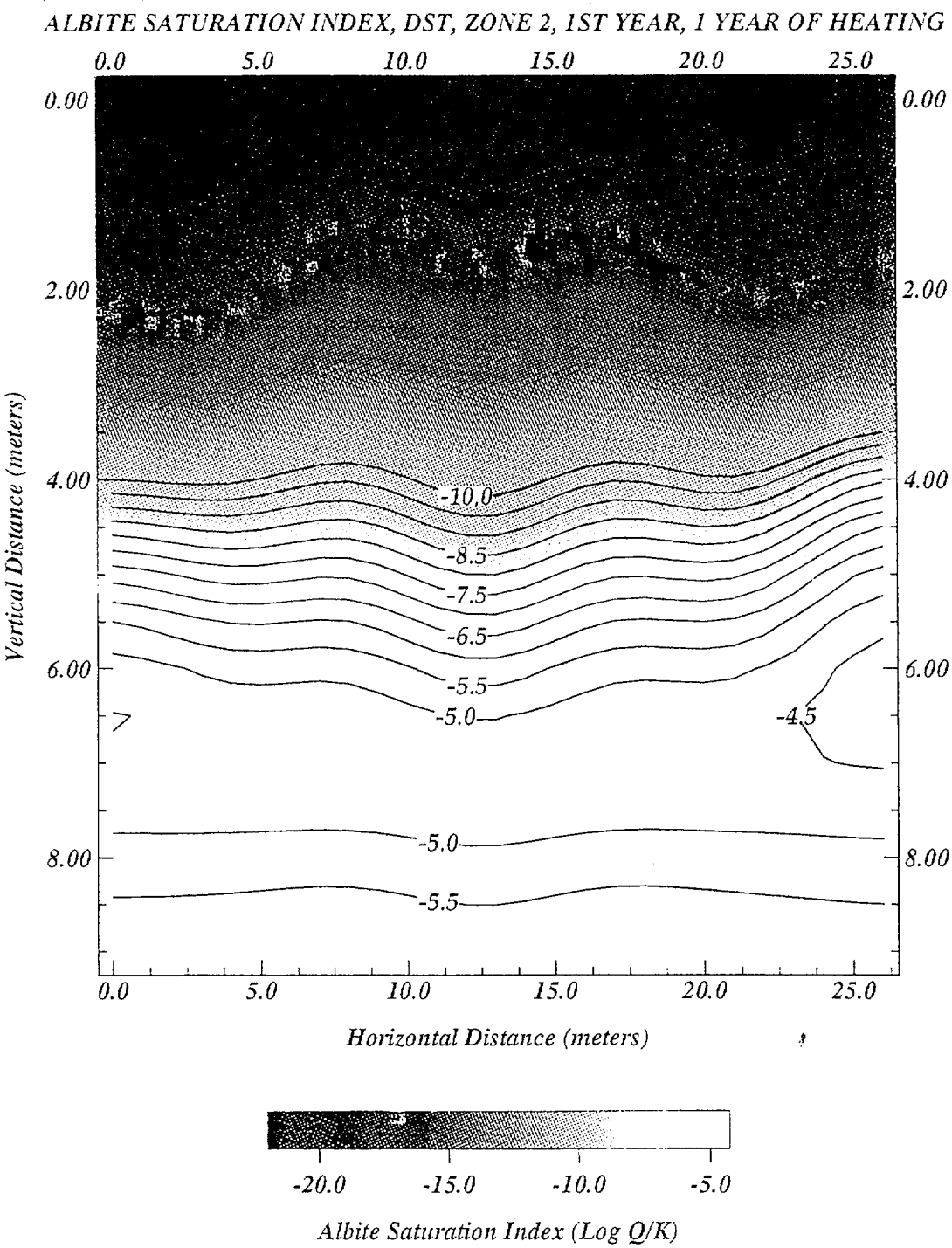
ALBITE SATURATION INDEX, DST, ZONE 2, 1ST YEAR, 1 YEAR OF HEATING
0.0
5.0
10.0
15.0
20.0
25.0
0.00
2.00
4.00
6.00
8.00
Vertical Distance (meters)
-10.0
-8.5
-7.5
-6.5
-5.5
-5.0
-4.5
-5.0
-5.5
Horizontal Distance (meters)
-20.0
-15.0
-10.0
-5.0
Albite Saturation Index (Log Q/K)

Figure 11a

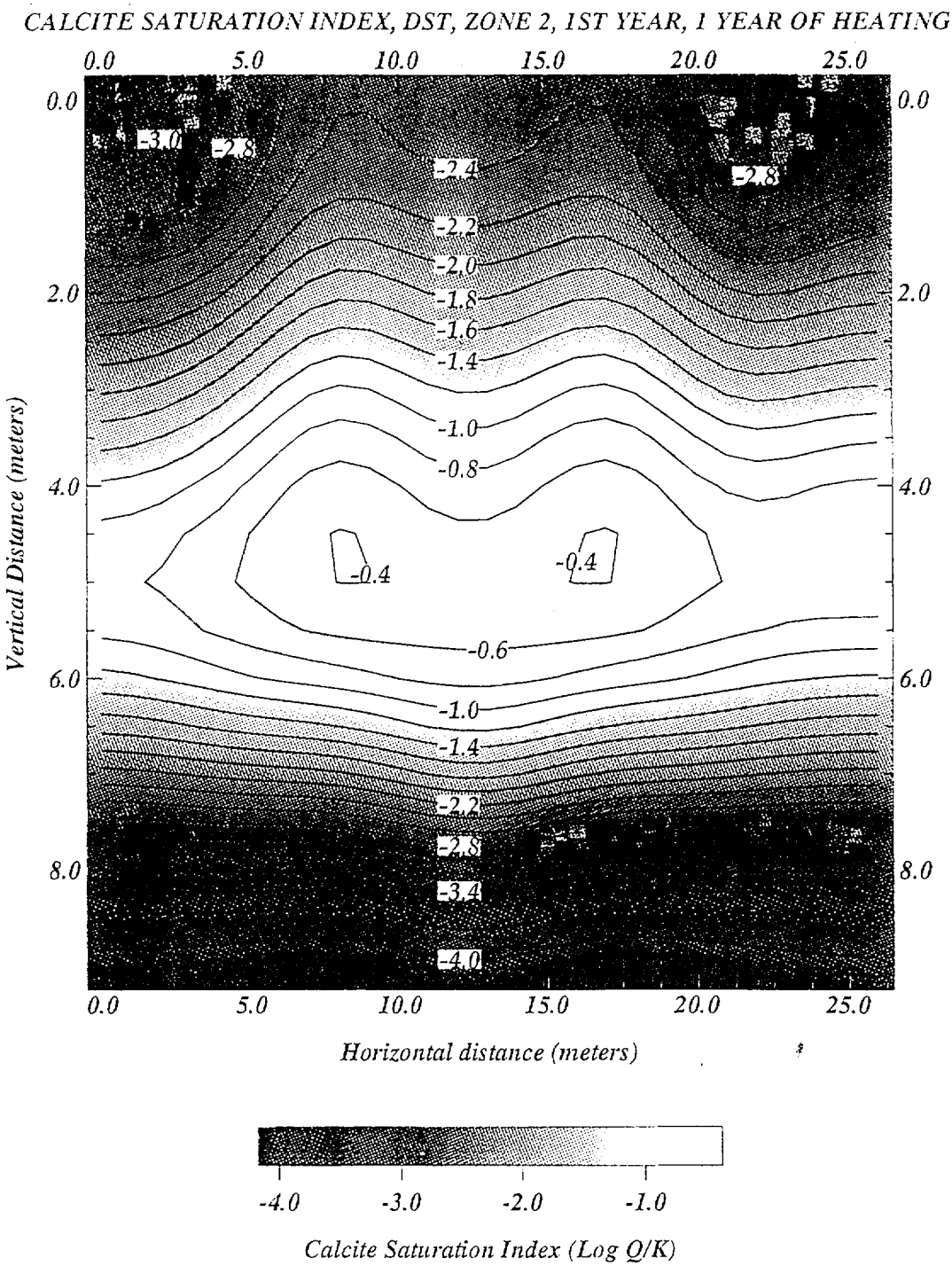
CALCITE SATURATION INDEX, DST, ZONE 2, 1ST YEAR, 1 YEAR OF HEATING
0.0
5.0
10.0
15.0
20.0
25.0
2.0
4.0
6.0
8.0
Vertical Distance (meters)
Horizontal distance (meters)
-2.4
-2.2
-2.0
-1.8
-1.6
-1.4
-1.0
-0.8
-0.4
-0.6
-3.4
-4.0
-4.0
-3.0
-2.0
-1.0
Calcite Saturation Index (Log Q/K)

Figure 11b

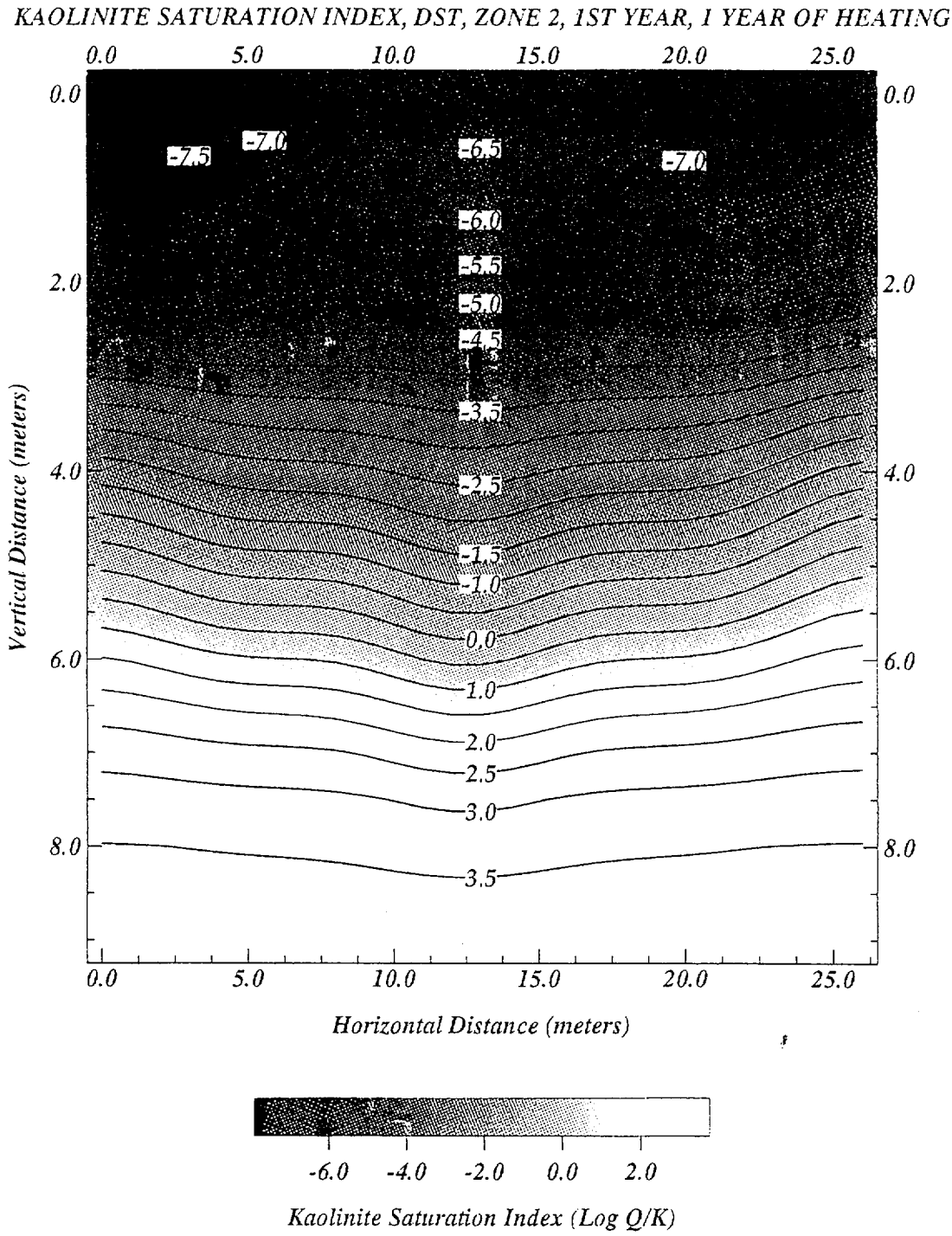
KAOLINITE SATURATION INDEX, DST, ZONE 2, 1ST YEAR, 1 YEAR OF HEATING
0.0
5.0
10.0
15.0
20.0
25.0
2.0
4.0
6.0
8.0
Vertical Distance (meters)
-7.5
-7.0
-6.5
-6.0
-5.5
-5.0
-4.5
-3.5
-2.5
-1.5
-1.0
0.0
1.0
2.0
2.5
3.0
3.5
Horizontal Distance (meters)
-6.0
-4.0
-2.0
0.0
2.0
Kaolinite Saturation Index (Log Q/K)

Figure 11c

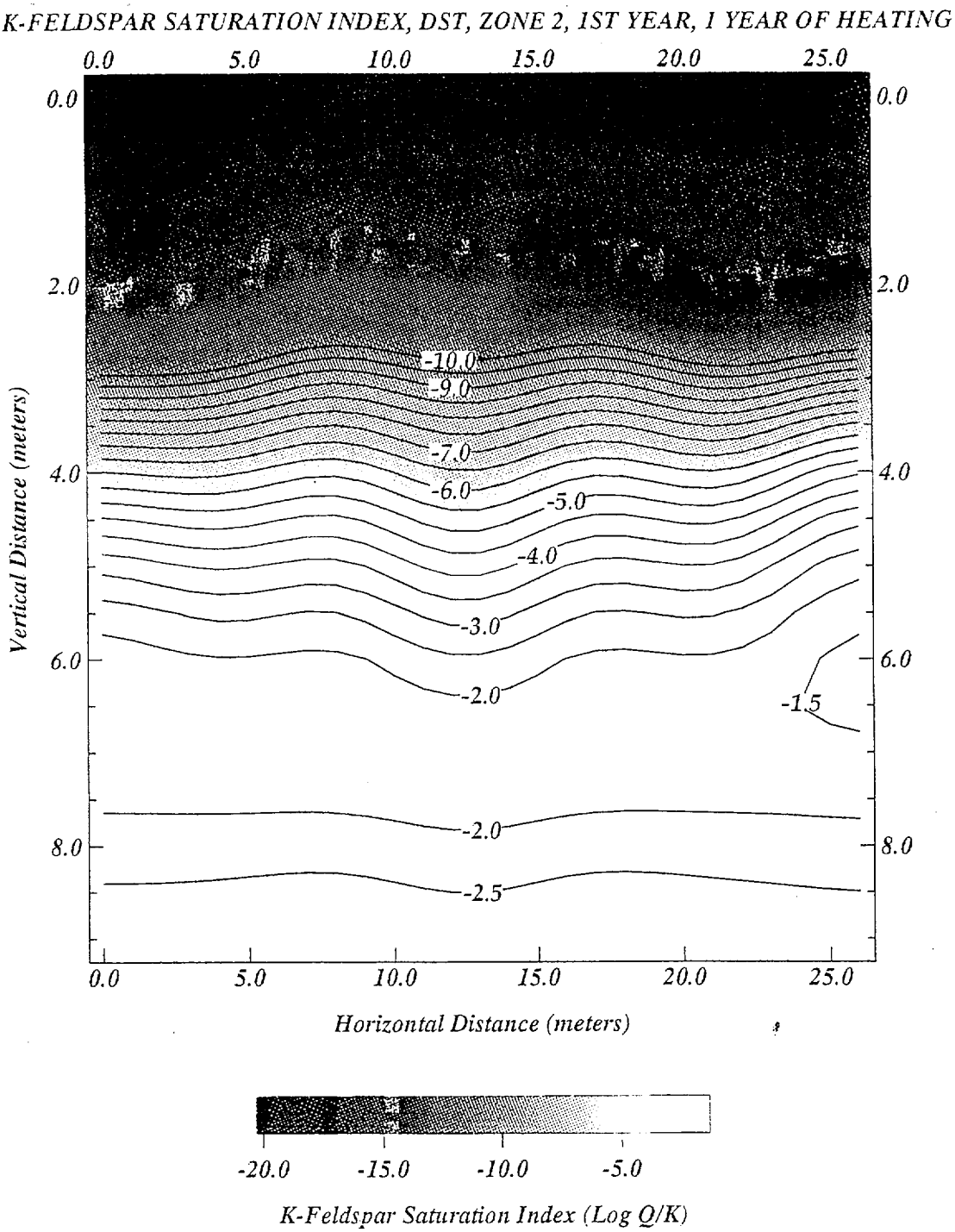
K-FELDSPAR SATURATION INDEX, DST, ZONE 2, 1ST YEAR, 1 YEAR OF HEATING
0.0
5.0
10.0
15.0
20.0
25.0
0.0
2.0
4.0
6.0
8.0
Vertical Distance (meters)
-10.0
-9.0
-7.0
-6.0
-5.0
-4.0
-3.0
-2.0
-1.5
-2.0
-2.5
Horizontal Distance (meters)
-20.0
-15.0
-10.0
-5.0
K-Feldspar Saturation Index (Log Q/K)

Figure 11d

QUARTZ SATURATION INDEX, DST, ZONE 2, 1 YEAR OF HEATING

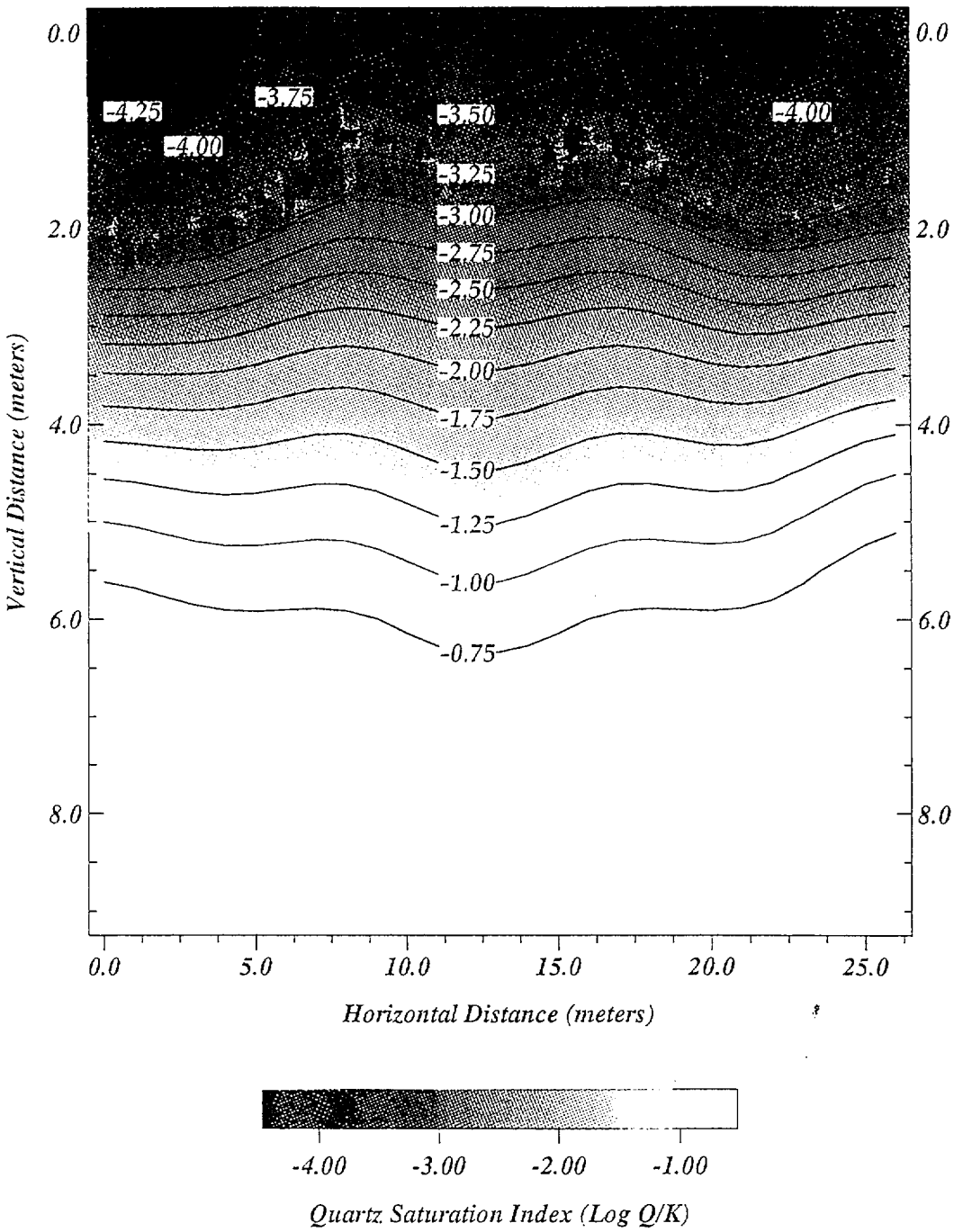

Figure 11e

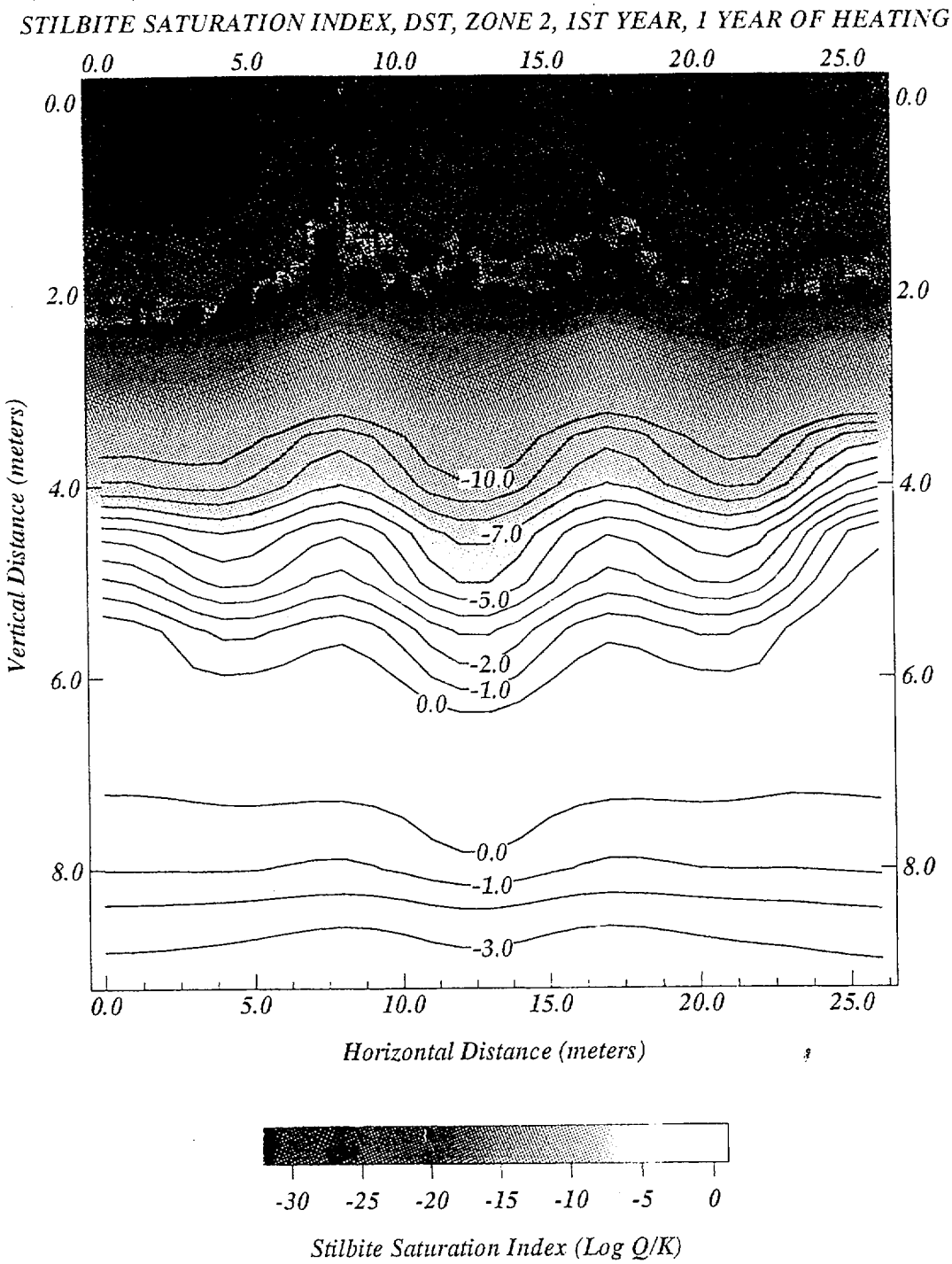
STILBITE SATURATION INDEX, DST, ZONE 2, 1ST YEAR, 1 YEAR OF HEATING
0.0
5.0
10.0
15.0
20.0
25.0
2.0
4.0
6.0
8.0
Vertical Distance (meters)
-10.0
-7.0
-5.0
-2.0
-1.0
0.0
0.0
-1.0
-3.0
Horizontal Distance (meters)
-30
-25
-20
-15
-10
-5
0
Stilbite Saturation Index (Log Q/K)

Figure 11f

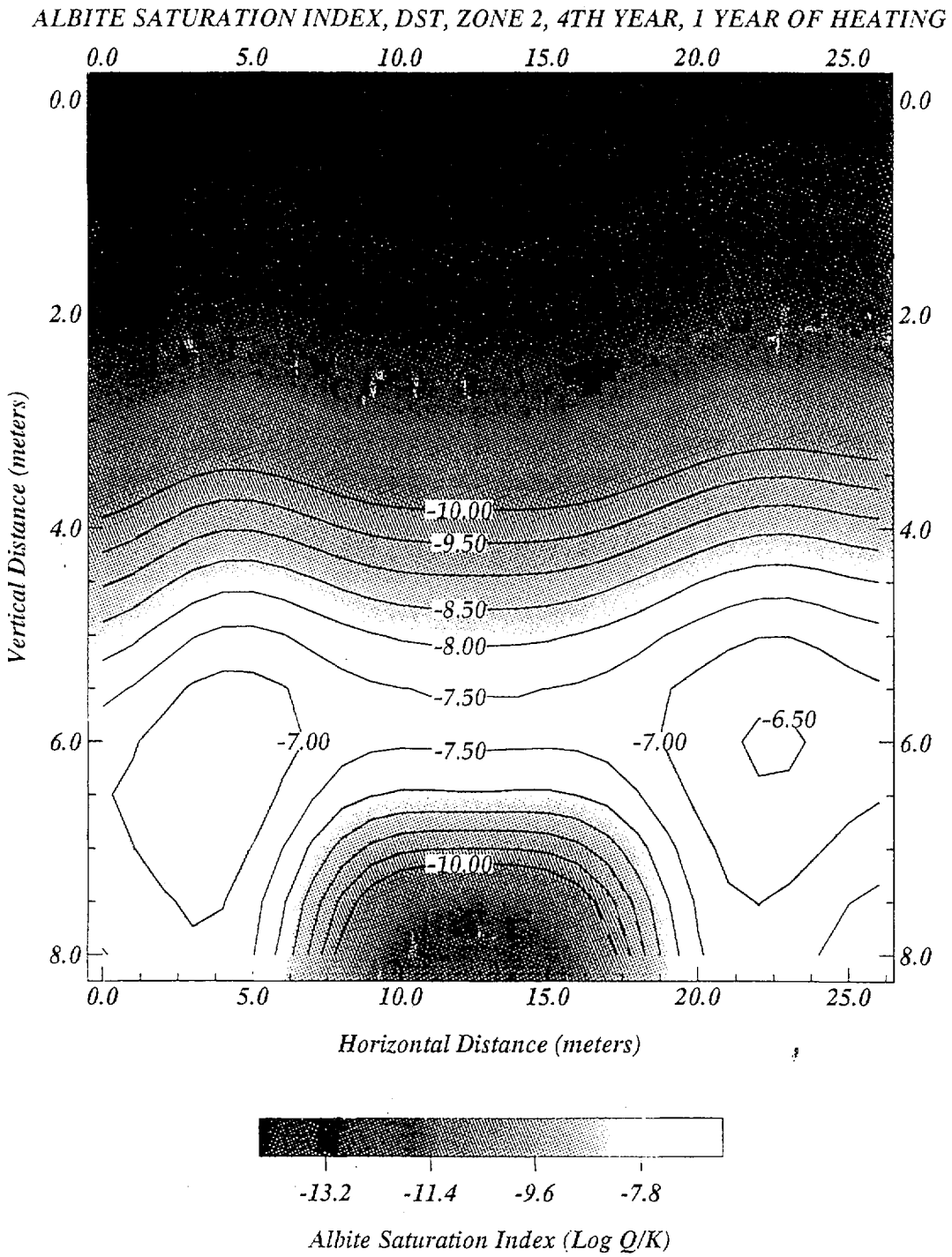
ALBITE SATURATION INDEX, DST, ZONE 2, 4TH YEAR, 1 YEAR OF HEATING
0.0
5.0
10.0
15.0
20.0
25.0
2.0
4.0
6.0
8.0
Vertical Distance (meters)
-10.00
-9.50
-8.50
-8.00
-7.50
-7.00
-7.50
-7.00
-6.50
-10.00
Horizontal Distance (meters)
-13.2
-11.4
-9.6
-7.8
Albite Saturation Index (Log Q/K)

Figure 12a

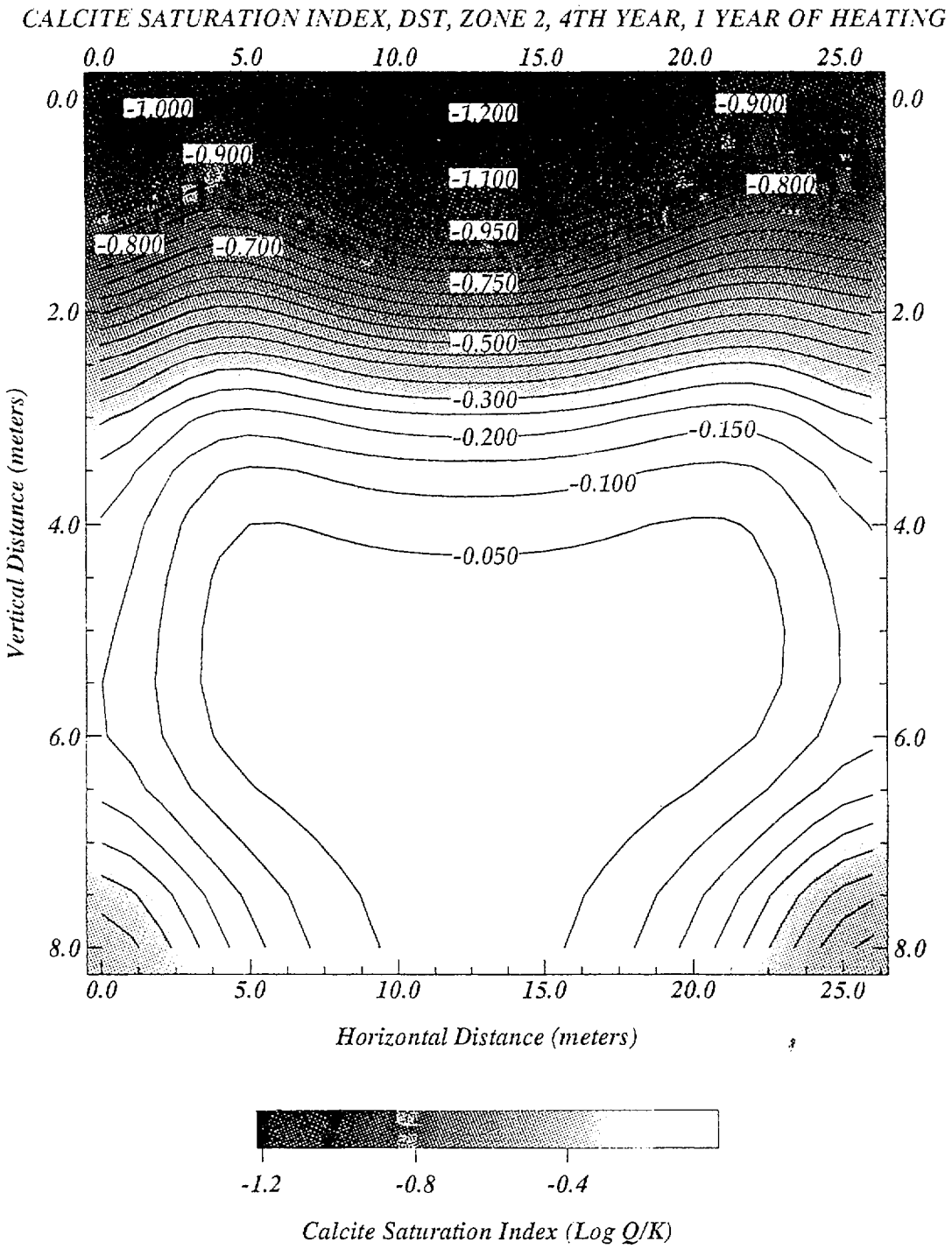
CALCITE SATURATION INDEX, DST, ZONE 2, 4TH YEAR, 1 YEAR OF HEATING
0.0
5.0
10.0
15.0
20.0
25.0
2.0
4.0
6.0
8.0
-1.000
-1.200
-0.900
-0.900
-1.100
-0.800
-0.800
-0.700
-0.950
-0.750
-0.500
-0.300
-0.200
-0.150
-0.100
-0.050
Vertical Distance (meters)
Horizontal Distance (meters)
-1.2
-0.8
-0.4
Calcite Saturation Index (Log Q/K)

Figure 12b

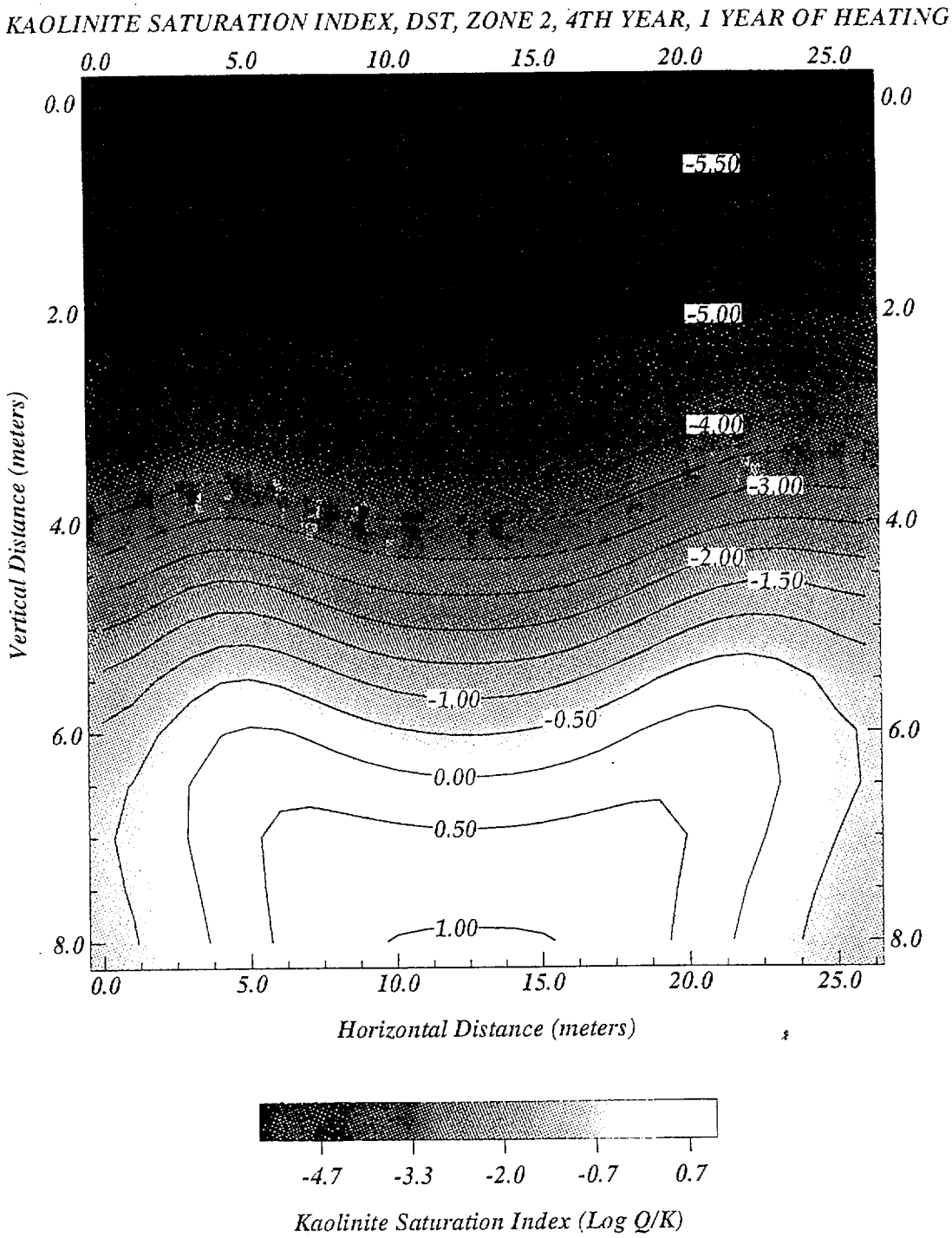
KAOLINITE SATURATION INDEX, DST, ZONE 2, 4TH YEAR, 1 YEAR OF HEATING
0.0
5.0
10.0
15.0
20.0
25.0
2.0
4.0
6.0
8.0
Vertical Distance (meters)
Horizontal Distance (meters)
-5.50
-5.00
-4.00
-3.00
-2.00
-1.50
-1.00
-0.50
0.00
0.50
1.00
-4.7
-3.3
-2.0
-0.7
0.7
Kaolinite Saturation Index (Log Q/K)

Figure 12c

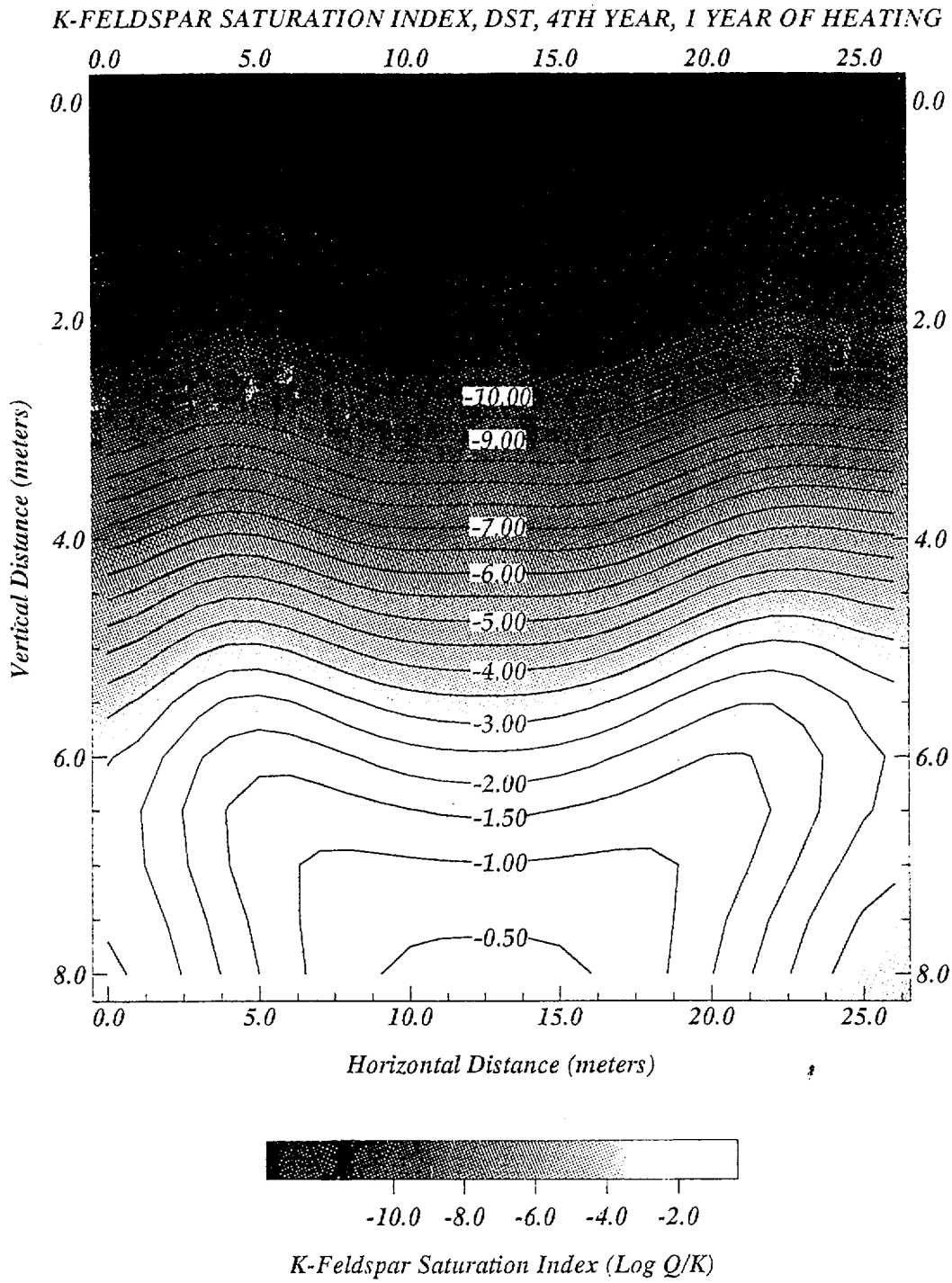
K-FELDSPAR SATURATION INDEX, DST, 4TH YEAR, 1 YEAR OF HEATING
0.0
5.0
10.0
15.0
20.0
25.0
2.0
4.0
6.0
8.0
Vertical Distance (meters)
-10.00
-9.00
-7.00
-6.00
-5.00
-4.00
-3.00
-2.00
-1.50
-1.00
-0.50
Horizontal Distance (meters)
-10.0
-8.0
-6.0
-4.0
-2.0
K-Feldspar Saturation Index (Log Q/K)

Figure 12d

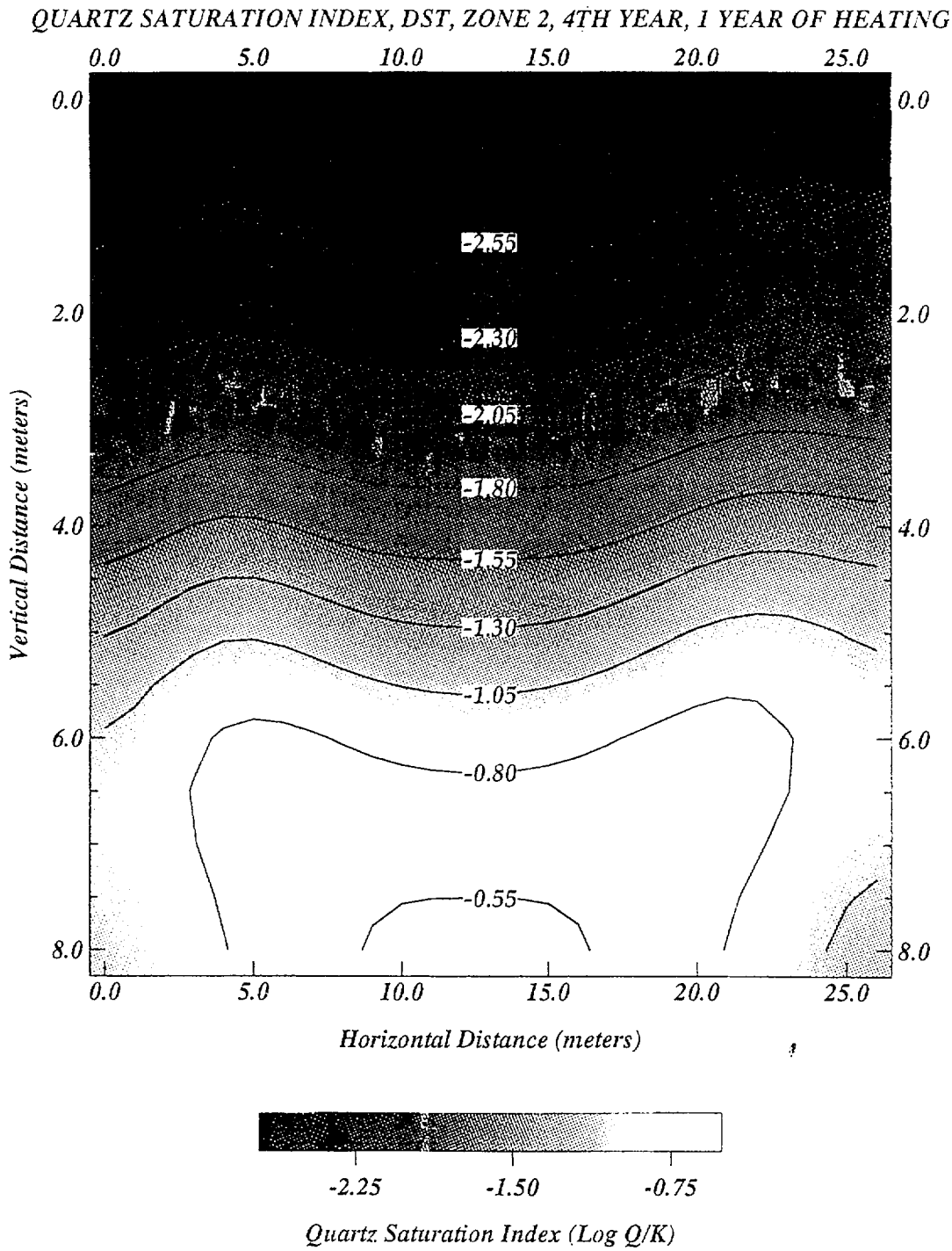
QUARTZ SATURATION INDEX, DST, ZONE 2, 4TH YEAR, 1 YEAR OF HEATING
0.0
5.0
10.0
15.0
20.0
25.0
0.0
2.0
4.0
6.0
8.0
Vertical Distance (meters)
-2.55
-2.30
-2.05
-1.80
-1.55
-1.30
-1.05
-0.80
-0.55
Horizontal Distance (meters)
-2.25
-1.50
-0.75
Quartz Saturation Index (Log Q/K)

Figure 12e

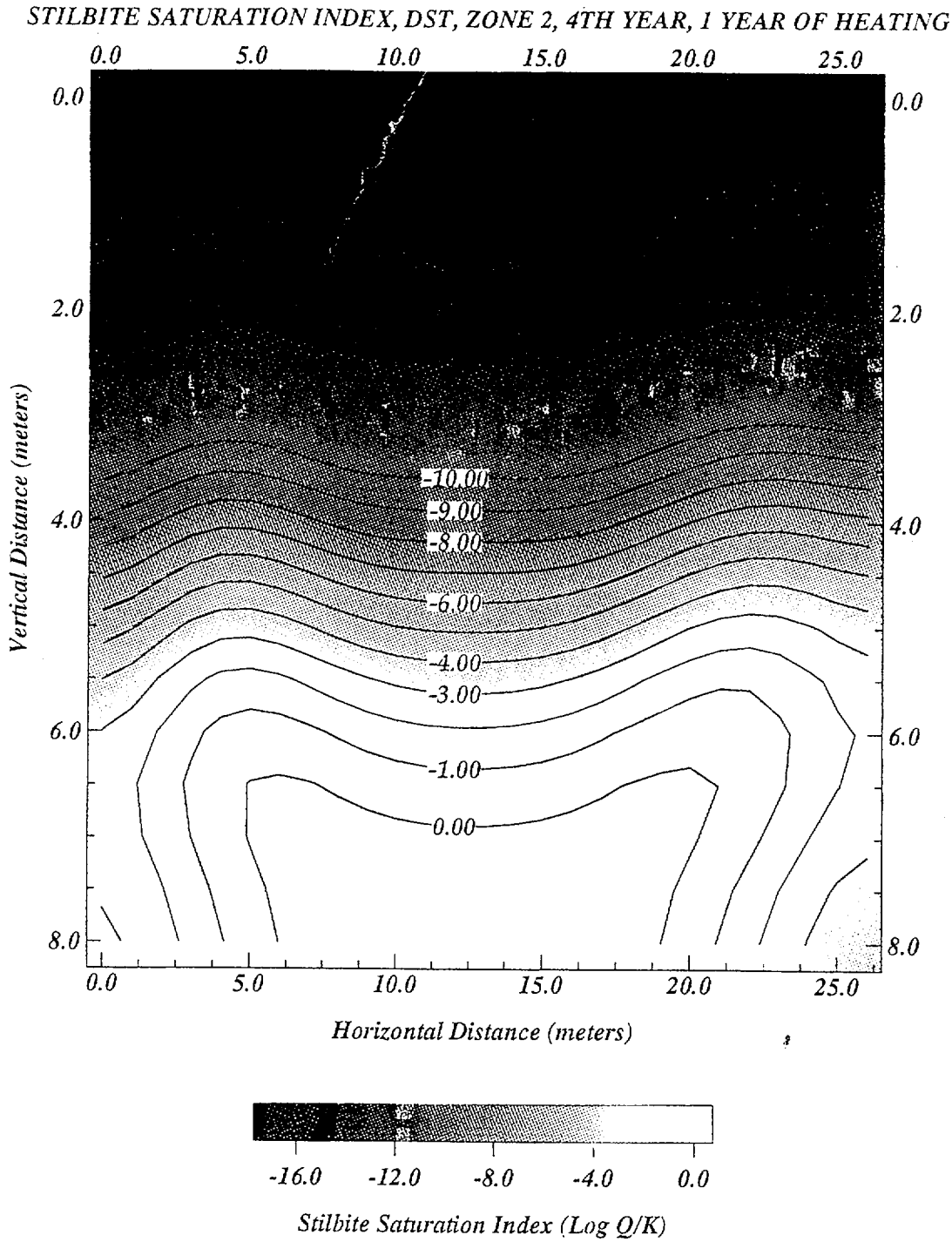
STILBITE SATURATION INDEX, DST, ZONE 2, 4TH YEAR, 1 YEAR OF HEATING
0.0
5.0
10.0
15.0
20.0
25.0
2.0
4.0
6.0
8.0
Vertical Distance (meters)
-10.00
-9.00
-8.00
-6.00
-4.00
-3.00
-1.00
0.00
Horizontal Distance (meters)
-16.0
-12.0
-8.0
-4.0
0.0
Stilbite Saturation Index (Log Q/K)

Figure 12f